Life Sciences 239 (2019) 116869

Contents lists available at ScienceDirect

Life Sciences

journal homepage: www.elsevier.com/locate/lifescie

TLR4 signaling modulation of PGC1-α mediated mitochondrial biogenesis in the LPS-Chronic mild stress model: Effect of fluoxetine and pentoxiyfylline

L.H. Khedr[a,*], N.N. Nassar[b], Laila Rashed[d], E.D. El-denshary[b], A.M. Abdel-tawab[c]

[a] Departmment of Pharmacology, Faculty of Pharmacy, Misr International University, Cairo, Egypt
[b] Department of Pharmacology, Faculty of Pharmacy, Cairo University, Cairo, Egypt
[c] Department of Pharmacology, Faculty of Medicine, Ain Shams University, Cairo, Egypt
[d] Department of Biochemistry, Faculty of Medicine, Cairo University, Cairo, Egypt

ARTICLE INFO

Keywords:
LPS
CMS
TLR4/NFκB
PGC1-α
Mitochondrial biogenesis
AMPK

ABSTRACT

Aim: The addition of repeated lipopolysaccharide (LPS) to chronic mild stress was recently proposed in our lab as an alternative model of depression, highlighting the possible interaction between stress and immune-inflammatory pathways in predisposing depression. Given that CMS-induced depressive behavior was previously related to impaired hippocampal energy metabolism and mitochondrial dysfunction, our current study aimed to investigate the interplay between toll-like receptor 4 (TLR4) signaling and peroxisome proliferator-activated receptor gamma coactivators-1-alpha (PGC1-α) as a physiological regulator of energy metabolism and mitochondrial biogenesis in the combined LPS/CMS model.

Main methods: Male Wistar rats were exposed to either LPS (50 μg/kg i.p.) over 2 weeks, CMS protocol for 4 weeks or LPS over 2 weeks followed by 4 weeks of CMS (LPS/CMS). Three additional groups of rats were exposed to LPS/CMS protocol and treated with either pentoxifylline (PTX), fluoxetine (FLX) or a combination of both. Rats were examined for behavioral, neurochemical, gene expression and mitochondrial ultra-structural changes.

Key findings: LPS/CMS increased the expression of TLR4 and its downstream players; MyD88, NFκB and TNF-α along with an escalation in hippocampal-energy metabolism and p-AMPK. Simultaneously LPS/CMS attenuated the expression of PGC1-α/NRF1/Tfam and mt-DNA. The antidepressant (AD) 'FLX', the TNF-α inhibitor 'PTX' and their combination ameliorated the LPS/CMS-induced changes. Interestingly, all the aforementioned changes induced by the LPS/CMS combined model were significantly less than those induced by CMS alone.

Significance: Blocking the TLR4/NFκB signaling enhanced the activation of the PGC1-α/NRF1/Tfam and mt-DNA content independent on the activation of the energy-sensing kinase AMPK.

1. Introduction

The brain is no longer considered isolated from the immune system. Rather, it relays signals via neural, humoral and blood-brain-barrier pathways consequent to systemic immune responses [1]. Immune/inflammatory activation and stress biomarkers are causal effectors mediating changes in brain structures and functions via alteration of neurotransmitter metabolism, neuroendocrine and mitochondrial functions [2–9].

Experimental models of stress and depression underscored the association of defective energy metabolism, altered mitochondrial ATP production as well as the inhibition of mitochondrial respiratory chain complexes along with depressive behavior [10–14]. The role of mitochondria as signal-processing center is not just restricted to cell death and survival, it rather brings in resilience to stress via modulation of mitochondrial biogenesis [15–17]. Recent research has identified several stress-regulated pathways that affect mitochondrial biogenesis through modulation of the activity of PGC-1α, a key sensor of cellular stress and regulator of mitochondrial biogenesis, which makes targeting PGC-1α as a proposed therapeutic option for several MDD pathologies associated with stress [18].

The concept of "leaky gut" in the pathophysiology of MDD was proposed as a trigger to a cascade of amplifications in the immune pathways [19]. Similarly, Garate et al., reported that CMS exposure enhanced the intestinal permeability and the translocation of LPS from Gram-negative bacteria to the systemic circulation thus, activating the innate immune cells, [20]. The Activation of the peripheral innate immune cells enhances the secretion of PICs [21,22] which target

* Corresponding author. Department of Pharmacology, Faculty of Pharmacy, Misr International University, KM 28 Cairo – Ismailia Road Ahmed Orabi District, Cairo, Egypt.
E-mail address: lobna.hatem@miuegypt.edu.eg (L.H. Khedr).

https://doi.org/10.1016/j.lfs.2019.116869
Received 1 February 2019; Received in revised form 10 September 2019; Accepted 10 September 2019
Available online 31 October 2019
0024-3205/

List of non-standard abbreviations

ADs	Antidepressants
AEC	Adenylate energy charge
CORT	Corticosterone
CMS	Chronic mild stress
C.SAL	Control group receiving saline
C.FLX	Control group receiving fluoxetine
C.PTX/FLX	Control group receiving both pentoxifylline and fluoxetine
FLX	Fluoxetine
FST	Forced swim test
GR	Glucocorticoid receptor
LPS	Lipopolysaccharide
MDD	Major depressive disorder
MyD88	Myeloid differentiation primary response 88
NRF1	Nuclear respiratory factor 1
OFT	Open-field test
PAMP	Pathogen-associated molecular patterns
p-AMPK	Phosphorylated AMP kinase
PGC1-α	Peroxisome proliferator-activated receptor gamma coactivators 1 alpha
PICs	Proinflammatory cytokines
PTX	Pentoxifylline
SAL	Saline
SP	Sucrose preference
SPT	Sucrose preference test
TNF-α	Tumor necrosis factor alpha
TAN	Total adenine nucleotides
TFAM	Mitochondrial transcription factor A
TLR	Toll-like receptor
mt-DNA	Mitochondrial DNA

neuronal substrates and elicit a "sickness behavior" that usually evolves into depressive-like behavior after LPS administration [1,23,24], offering a convincing face validity for the endotoxin-induced behavioral changes as an animal model of depression [23]. Notably, chronic treatment with ADs ameliorated the LPS-induced depressive-like behavior in rats [25–28], thus ascribing more predictive validity to the LPS-induced anhedonia as an animal model of depression.

Additionally, CMS enhanced the expression of TLR4 in brain tissue following translocation of intestinal LPS [20]. Thus, in depression, the interaction between the effects of LPS derived from leaky gut and psychological stress-induced up-regulation of TLRs might be expected [29]. Precisely, there is a reasonable evidence that TLR4 is highly expressed in patients with MDD [30,31] and this elevated expression was responsive to different treatments that ended up into improvement in depressive symptoms, hence, attributing TLR4 activity in the pathophysiology of MDD [4]. Peripheral administration of LPS, a TLR4 ligand, is the frequently used immunological challenge in animal models of cytokine-induced depression [32,33].

The AD 'FLX' was recently reported to significantly attenuate the LPS-induced despair behavior and hippocampal neuroinflammation [34]. Similarly, 'PTX', a blocker of TNF-α synthesis [35], was reported to reverse the effects of both CMS and LPS in rats [25,36].

The current investigation aimed at exploring interplay between TLR4/NFκB signaling and PGC1-α mediated mitochondrial biogenesis as well as the potentials of the AD "FLX" and the anti TNF-α "PTX" singly or in combination to ameliorate the LPS/CMS induced changes.

2. Materials and methods

2.1. Animals

One hundred and thirty-eight adult male Wistar rats (The Nile Company for Pharmaceutical Industries, Cairo, Egypt) weighing (200–250 g) were housed individually with pelleted rat chow (Meladco chow, El Obour, Egypt) and tap water available *ad libitum* for the duration of the experiments, unless otherwise was recommended by the study protocol. Animals were allowed to acclimatize to the surroundings before any experimentation for at least 2 weeks. Temperature was maintained at 22 ± 2 °C. A reversed light-dark cycle[1] was held at 12:12 h with lights on at 5:00 p.m. and off at 5:00 a.m., starting from the beginning of the acclimatization period, unless otherwise was recommended by the study protocol. Consequently, all the maneuverings of the study were performed during the 'arranged' dark cycle. All handling was performed by the same investigator throughout the studies. Experimental protocols were approved by the Research Ethical Committee of Faculty of Pharmacy Cairo University ***[REC-FOPCU/serial number PT (730), 29/4/2013]*** and comply with the Guide for the Care and Use of Laboratory Animals **(ILAR 1996)** [37]. All efforts were made to minimize the number of animals used and their suffering.

[1] The fact that rats are night dwellers (most of their activities are in the dark cycle of the dark/light transitions), underlined the logic of reversing the cycles to allow the experimental maneuvers to be during their utmost activity and at the convenience of lab routine.

2.2. Treatments

LPS (Escherichia coli serotype O55:B5), PTX and FLX were purchased from Sigma-Aldrich (St Louis, MO, USA). Drugs solutions were freshly prepared by dissolving compounds in sterile endotoxin-free isotonic saline and administered i.p. in a volume of 1 ml/kg (LPS) or 2 ml/kg (PTX and FLX). LPS was administered at a dose 50 μg/kg, this dose was chosen after an efficacy check in our lab [25]; regarding its ability to induce a significant increase in the despair behavior in the forced swim test (FST). PTX was administered at a dose of 100 mg/kg following an initial pilot study; comparing the effectiveness of 50, 100 and 150 mg/kg in attenuating the LPS induced increase in serum TNF-α. FLX was administered at a dose of 10 mg/kg [38].

2.3. Experimental design

2.3.1. Groups' distribution

The studied groups were intended to be interpreted on two comparison levels as presented in **(**Fig. 1**).**

2.3.1.1. Level A: effects of single and combined stressful exposures. This comparative level was composed of five groups:

(1) **C.SAL** *(n = 11):* Control rats, received a daily i.p. injection of saline (0.5 ml/kg) for 6 weeks and examined by the end of the 6th week.
(2) **SAL/CMS** *(n = 16)*: received i.p. injection of saline (0.5 ml/kg) every other day over 2 weeks *(a total of 6 doses)*, followed by exposure to CMS protocol **(**Table 1**)** and continued with i.p. saline (0.5 ml/kg) for another four weeks.
(3) **LPS/SAL** *(n = 11)*: received LPS every other day (a total of six doses) over 2 weeks, followed by a daily i.p. injection of saline (0.5 ml/kg) for another four weeks and thereafter examined by the end of the 6th week.
(4) **LPS/CMS** *(n = 18)*: received LPS every other day (a total of six doses) over 2 weeks, followed by exposure to CMS protocol **(**Table 1**)** while being injected daily with saline (0.5 ml/kg) i.p. for another four weeks.

2.3.1.2. Level B: effects of FLX and PTX individually or in combination, on

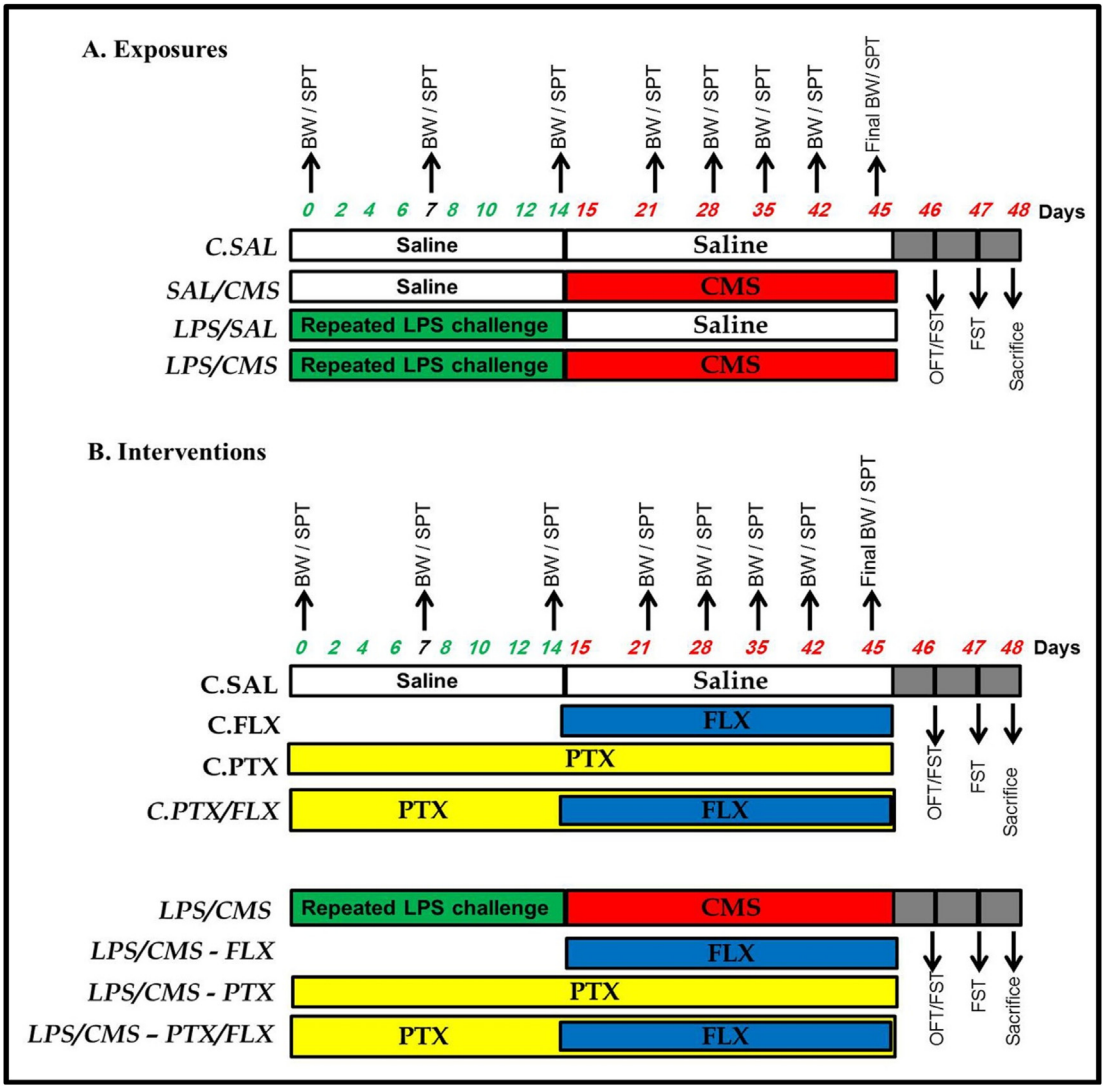

Fig. 1. Schema for the combined LPS/CMS model and PTX, FLX (singly or combined) treatment schedule, behavioral experiments, and decapitation.
Control animals were neither exposed to the LPS nor CMS. They were kept undisturbed in their home cages and administered the vehicle saline "daily". In the positive control groups; the non-stressed animals administered FLX, PTX or their combination in the same pattern as the stressed groups.
BW: body weight measurement; CMS: Chronic mild stress; FLX: Fluoxetine (10 mg/kg i.p); FST: Forced swim test; LPS: Lipopolysaccharides (50 μg/kg i.p, every other day, a total of six doses); OFT: Open-field test; PTX: Pentoxiphylline (100 mg/kg i.p); SPT: sucrose preference test; OFT: open field test.

the LPS/CMS combined model. In this comparison level, 8 groups were involved where the C.SAL and the LPS/CMS groups used in the previous comparison were further utilized in this comparison as well. The remaining groups involved included:

(1) **C.FLX** *(n = 9)*: positive control rats, received i.p. injections of saline (0.5 ml/kg) every other day over 2 weeks, followed *by* a daily i.p. injection of FLX for the last four weeks.
(2) **C.PTX** *(n = 11)***:** positive control rats, received i.p. injections of saline (0.5 ml/kg) every other day over 2 weeks, while treated daily with PTX for the whole 6 weeks.
(3) **C.PTX/FLX** *(n = 11)***:** positive control rats, received a saline i.p. injections (0.5 ml/rat) every other day over 2 weeks while treated daily with PTX, followed *by* a daily i.p. injections of PTX and FLX for another four weeks.
(4) **LPS/CMS-FLX** (n = 18)**:** received LPS every other day (a total of six doses) over 2 weeks, followed by exposure to CMS protocol (Table 1) while being treated with FLX for the last four weeks.
(5) **LPS/CMS-PTX** (n = 17)**:** received LPS every other day (a total of six doses) over 2 weeks followed by exposure to CMS protocol (Table 1) for another four weeks while being treated daily with PTX from the beginning of the LPS exposure till the end of the CMS schedule. In the first 2 weeks of LPS injections, rats received PTX 1 h before treatment with LPS [39,40].
(6) **LPS/CMS-PTX/FLX** (n = 16)**:** received LPS every other day (a total of six doses) over 2 weeks followed by exposure to CMS protocol (Table 1) for another four weeks while being treated daily with PTX from the beginning of the LPS exposure till the end of the CMS schedule and FLX during the last 4 weeks of the CMS exposure. Interventions were applied as in group 7.

2.4. Application of "CMS battery"

Rats were exposed to 2–5 mild stressors per day for 4 weeks, given that no more than 3 mild stresses were applied simultaneously (Table 1)**.** Stressors were applied in a quasi-random sequence over the course of a week and repeated in successive weeks, with slight shifting between the days (Khedr et al., 2015). Applied stressors included; water and/or food deprivation (water deprivation not exceeding 14 h), restricted food access (*i.e.* 2–3 chow pellets) after food deprivation, empty

Table 1
Schedule of stressors application during a period of one week.

Day	Dark cycle		Light cycle	
	Duration	Stressor	Duration	Stressor
Sat	***9am - 5pm***	Stroboscopic light	***5 p.m.- 9 a.m.***	Cage tilting Foreign body
Sun	***9am - 5pm***	Pairing Noise Cold restraint (30 min)	***5 p.m. - 9 a.m.***	Soiling the cage
Mon	***5am -5pm***	Food/water deprivation Soiling of the cage	***5 p.m. - 5:30pm*** ***6 p.m. - 9 a.m.***	Sucrose preference test Stroboscopic light Foreign body
Tues	***9am - 5pm*** ***9am -11am***	Water deprivation Empty bottles	***5 p.m. - 9 a.m.***	Cage tilting Foreign body
Wed	***9am - 5pm***	Pairing Noise Cold restraint (30 min)	***5 p.m. - 9 a.m.***	Food/water deprivation
Thurs	***9am - 5pm*** ***9am - 11am***	Stroboscopic light Foreign body Restricted food	***5 p.m. - 9 a.m.***	Reversed light/ dark cycle
Fri	Continuous illumination			

Slight variation in the stressors application was adopted to avoid habituation. Saturday and Sunday light cycle stressors were shifted every other week. Tuesday and Wednesday light cycle stressors were also shifted every other week except for the empty bottle stressor it was always on Tuesday.

water bottles after water deprivation, cage tilting, 24 h lighting, pairing, stroboscopic light, intermittent white noise (85 dB), cold temperature (≈10 °C) and soiling of the cage. Stressors were repeated each week for a total of four weeks. Control animals were kept undisturbed and in a separate room except of general handling (regular cage cleaning and measuring body weight).

2.5. Brain tissue sampling

Rats were euthanized using i.p. urethane (1.2 g/kg). Blood samples "retro orbital", were taken from the animals during the dark cycle in order minimize the effect of circadian rhythm on the results. The sera were separated within 1 h of blood collection and rapidly stored at −80 °C until further assay. The animals were further classified into two sets:

•***Set A:*** Used for biochemical and molecular analysis. Brains were immediately removed and the hippocampi were dissected under strict cooling conditions then flash frozen in methyl butane (cooled on dry ice). The dissected hippocampi were either; ***(i)*** stored at −80 °C until further assay for biochemical, HPLC analysis and mt-DNA content or ***(ii)*** placed in individual RNAase-free eppendorf tubes containing 300 µl of RLT buffer; a highly denaturing guanidine-thiocyanate-containing buffer supplied by the **RNeasy Mini Kit** (Qiagen, Hilden, Germany) which immediately inactivates ribonuclease **(**RNases) to ensure purification of intact RNA and stored at −80 °C for 24 h and then processed for molecular analysis *(vide infra)*. All the biochemical parameters were normalized to protein content, measured according to Bradford assay using the Bio-Rad protein assay reagent (Bio-RAD, Richmond, USA) according to the kit instruction manual using bovine serum albumin as a standard.

•***Set B:*** Used for the analysis of ultra-structural changes (mainly in the mitochondria) in the pyramidal neurons of the hippocampus *via* Transmission Electron Microscopy (TEM).

2.6. TLR4 signaling cascade and markers of mitochondria biogenesis

2.6.1. Real-time reverse transcription-polymerase chain reaction (RT-PCR)

Total RNA for TLR4 signaling cascade (TLR4; MyD88; NFκB) and markers of mitochondrial biogenesis (PGC1-α; NRF1; TFAM) was extracted from hippocampal tissue homogenates using RNeasy Mini Kit (Qiagen, Hilden, Germany) according to the manufacturer's instructions. Reverse transcription into cDNA was performed from the total isolated RNA using High Capacity cDNA Reverse Transcription Kit (Applied Biosystems, CA, USA) following the manufacturer's instructions. Rt-PCR reaction was performed using SYBR green PCR Master Mix (Applied Biosystems, CA, USA).

Table 2
Sequence of the primers for RT-PCR

Gene	Gene Accession no.	Primer	
TLR4	NM_019178.1	Forward	**5**-GCC GGA AAG TTA TTG TGG TGG T-**3**
		Backward	**5**-ATG GGT TTT AGG CGC AGA GTT T-**3**
MyD88	NM_198130	Forward	**5**-CAA CCA GCA GAA ACA GGA GTC T-**3**
		Backward	**5**-ATT GGG GCA GTA GCA GAT GAA G-**3**
NFκB	NM_199267	Forward	**5**-GCG CAT CCA GAC CAA CAA TAA C-**3**
		Backward	**5**-GCC GAA GCT GCA TGG ACA CT-**3**
PGC1-α	NM_031347	Forward	**5**-GTGCAGCCAAGACTCTGTATGG-**3**
		Backward	**5**-GTCCAGGTCATTCACATCAAGTTC-**3**
NRF1	NM_001100708	Forward	**5**-TTACTCTGCTGTGGCTGATGG-**3**
		Backward	**5**-CCTCTGATGCTTGCGTCGTCT-**3**
TFAM	NM_031326	Forward	**5**-GAAAGCACAAATCAAGAGGAG-**3**
		Backward	**5**-CTGCTTTTCATCATGAGACAG-**3**
mt-DNA	X14848.1	Forward	GGTTCTTACTTCAGGGCCATCA
		Backward	GATTAGACCCGTTACCATCGAGAT
β-Actin	NM_031144	Forward	**5**-GCC ATG TAC GTA GCC ATC CA-**3**
		Backward	**5**-GAA CCG CTC ATT GCC GAT AG-**3**

Total DNA for mt-DNA copy number analysis was isolated from freshly dissected hippocampus using Wizard Genomic DNA purification kit (Promega, Madison, USA) according to manufacturers' recommendations.

PCR reactions were set up in a total volume of 50 µl; containing 25 µl SYBR Green Mix (2x), 0.5 µl cDNA, 2 µl primer pair mix and 22.5 µl H2O. The forward and reverse primers were checked for correctness of the gene order according to the GenBank **(**Table 2**).** The relative expression of the studied genes was calculated after normalization to the internal standard β-Actin. All reactions were run on a StepOne™ Plus RealTime PCR system (Applied Biosystems) using the default settings recommended by the manufacturer, and analyzed using StepOne software v2.3.

2.6.2. Tissue TNF-α

The hippocampal TNF-α level were determined using the commercially available ELISA kit, R&D Systems (Minneapolis, USA). Absorbance was measured at 450 nm and the lowest analytical detectable level of was less than 5 pg/mL.

2.7. Energy metabolism

2.7.1. Adenine nucleotides and their metabolic ratios

Frozen hippocampal samples were homogenized in (1200 µl of ice-cold 0.76 M perchloric acid to which another 800 µl of 0.5 M perchloric acid containing 160 µM IMP as an internal standard) using an ice-chilled glass homogenizer, the homogenate was then allowed to extract for 30 min in ice-cold temperature, followed by centrifugation (6000 r.p.m. × 30 min at 4 °C). The supernatant was removed and neutralized by the addition of approximately 200 µl of 6 N KOH, controlling the pH with pH indicator strip. Any further precipitate appearing after neutralization was removed by centrifugation (6000 r.p.m. × 30 min at 4 °C). The collected supernatant was further filtrated using a 0.45 µm filter and used for direct analysis of energy metabolites. Samples (20 µl) after suitable pretreatment were submitted to isocratic HPLC using a reversed-phase octadecyl silane (C18) partition column (Alltech's 150 mm long x 4.6 mm internal diameter, 5.0 µm particle size, preceded by a short (40 × 4 mm) guard column of same material) at 37 °C. Flow rate was adjusted at 1 ml/min. Inosine-3-

monophosphate disodium salt (IMP) served as an internal standard. Mobile Phase comprised 20 mM potassium phosphate buffer pH 6. The nucleotides' peaks were analyzed spectrophotometricaly 254 = ʌnm and identified by comparison with the retention time of the corresponding standard solutions [11,41]. Method validation was carried out.

The concentration of ATP, ADP, and AMP in each sample was calculated from the calibration curve and expressed as nmol/mg protein. Subsequently ATP/ADP ratio and total adenine nucleotides (TAN = [ATP] + [ADP] + [AMP]) were calculated. Adenylate energy charge 'AEC' was further calculated according to (Atkinson, 1968): AEC = [ATP] + 1/2 [ADP])/TAN .

Notably AEC is considered a quantitative assessment of the cellular energy status; where it represents the amount of the metabolically available energy stored in the TAN pool [42]. Hence, the observed reduction in AEC seen may indicate high metabolic stress. Noteworthy, an AEC < 0.5 is indicative of cell death while values ranging from 0.55 to 0.75 indicate consumption of energy for defense mechanisms against stress [43]. Consequently, it is expected that in the presence of any metabolic stress and higher energy requirement, that cells will react with a depletion of ATP and a simultaneous increase in the ADP levels leading to a significant decrease in AEC [44].

2.7.2. p-AMPK

The metabolic fuel gauge 'AMPK' senses changes in the intracellular AMP/ATP ratio. Consequently, a rise in the AMP/ATP ratio would activate AMPK by phosphorylation. The activated AMPK (p-AMPK) acts to maintain cellular energy stores, switching on the catabolic pathways that produce ATP while switching off anabolic pathways that consume ATP [45].

The p-AMPK level was determined using the commercially available ELISA kit, Rat Phosphorylated adenosine monophosphate activated protein kinase, AMPK ELISA Kit (code number: 201-11-0437 Gentaur, Kampenhout, Belgium) according to the kit's instruction. Briefly, hippocampal samples were homogenized in phosphate buffer saline using an IKA T-10 Ultra-Turrax (Staufen, Germany) then centrifuged for 20 min at 3000 r.p.m using the cooling centrifuge (Sigma 3–30ks, Osterode, Germany). The supernatant was removed and loaded to the wells pre-coated with p-AMPK monoclonal antibody and processed according to the kit instruction manual. The absorbance was measured at 450 nm and the lowest analytical detectable level of was 0.482 ng/ml.

2.8. Serum biomarkers (CORT and TNF-α)

Blood samples were taken from the animals at the beginning of the

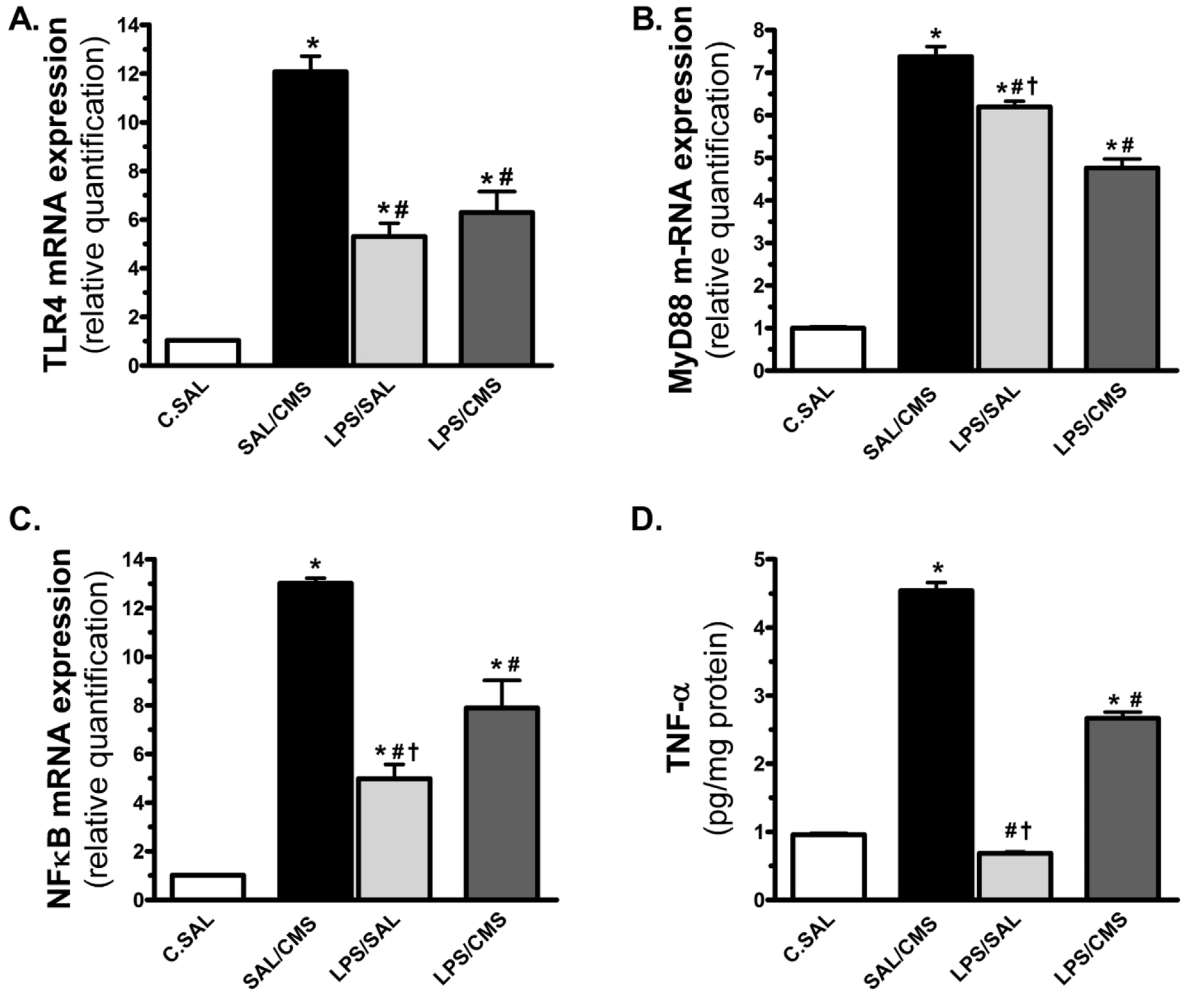

Fig. 2. Effects of LPS, CMS (separate or combined) on TLR4 expression and signaling
Bar graphs illustrating changes in: **(A)** TLR4, **(B)** MyD88, **(C)** NFκB and **(D)** TNF-α relative gene expression. Data are presented as mean ± S.E.M (n = 6–7). For comparisons among groups, one-way ANOVA followed by the post hoc "Tukey's Multiple Comparison Test" was utilized. *$p < 0.01$ significant in comparison C.SAL, $^{\#}p < 0.001$ significant in comparison to SAL/CMS, $^{\dagger}p < 0.05$ significant in comparison to the LPS/CMS. **TLR4**: Toll like receptor 4; **MyD88:** Myeloid differentiation primary response 88**; NFκB:** Nuclear factor kappa-B**;TNF-α:** Tissue tumor necrosis factor α; **C.SAL:** Control saline; **LPS:** Lipopolysaccharides (50 μg/kg i.p., every other day, a total of six doses); **CMS:** Chronic mild stress (4 weeks).

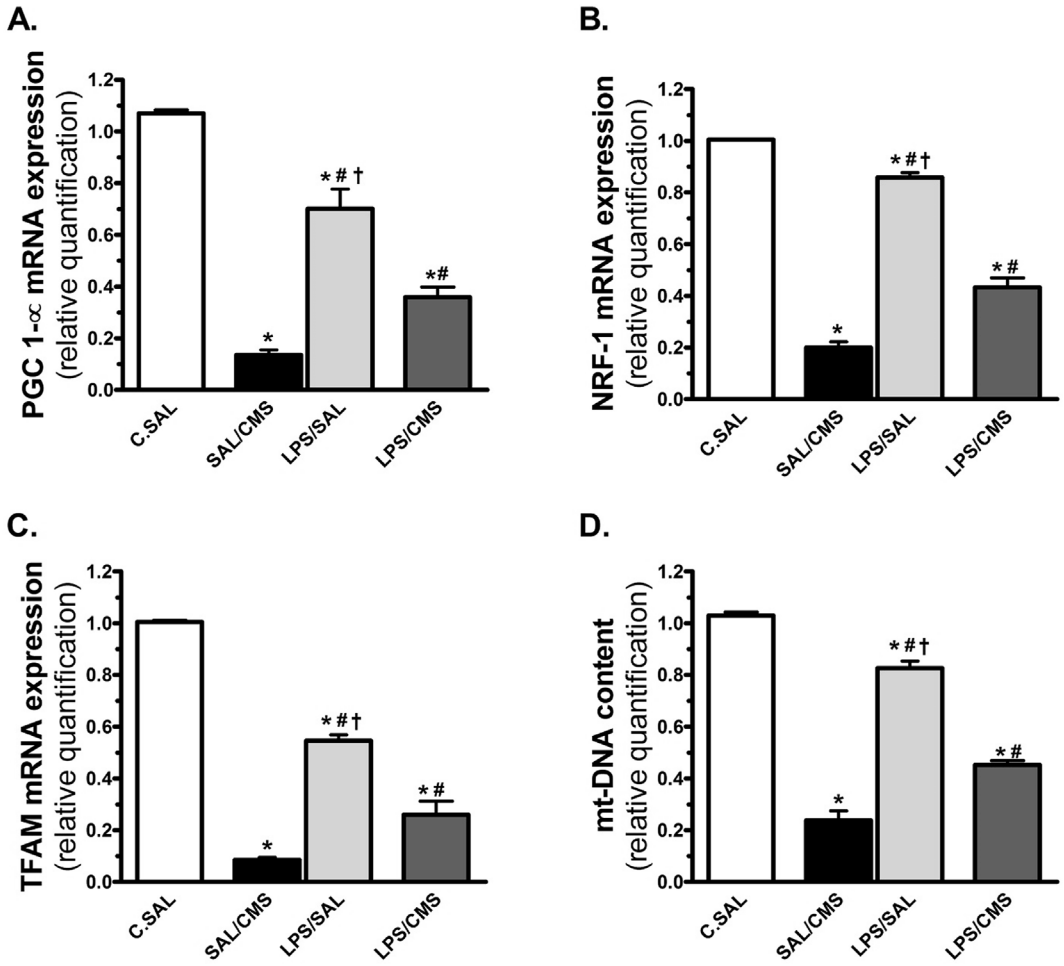

Fig. 3a. Effects of LPS, CMS (separate or combined) on the relative expression of mitochondrial biogenesis markers
Bar graphs illustrating changes in the relative expression of: **(A)** PGC1-α, **(B)** NRF-1, **(C)** TFAM and **(D)** mt-DNA content. Data are presented as mean ± S.E.M (n = 6–7). For comparisons among groups, one-way ANOVA followed by the post hoc "Tukey's Multiple Comparison Test" was utilized. $^{*}p < 0.01$ significant in comparison to C.SAL, $^{\#}p < 0.01$ significant in comparison to SAL/CMS, $^{\dagger}p < 0.001$ significant in comparison to the LPS/CMS.
PGC1-α: Peroxisome proliferator-activated receptor gamma coactivators 1 α, **NRF-1:** Nuclear respiratory factor 1**; TFAM:** Mitochondrial transcription factor A; **mt-DNA:** mitochondrial DNA; **C.SAL**: Control saline; **LPS:** Lipopolysaccharides (50 μg/kg i.p., every other day, a total of six doses); **CMS:** Chronic mild stress (4 weeks).

dark cycle and sera were separated and stored at −20°C until further assayed. Serum levels of CORT and TNF-α were determined using the commercially available ELISA kits; Corticosterone Rat/Mouse ELISA (DRG international®, USA), and Rat TNF-α Platinum ELISA (eBioscience, CA, USA) according to the manufacturer's instructions. Absorbance was measured at 450 nm and the lowest analytical detectable levels of CORT and TNF-α were (4.1 ng/ml and 11 pg/ml, respectively).

2.9. Weight gain and behavioral tests

All behavioral tests were constructed at least 24 h after the last stressor at the end of the experimental period. SPT was done weekly *"data not shown"* and at the end of the experiment. The sequence of applying the behavioral tests was; SPT, open-field test (OFT), then the FST, which was preceded one day with FST training. The Animals were sacrificed on the next day morning.

2.9.1. Final weight gain

Change in final weight gain was calculated as the difference between the final and baseline body weight. Weekly weight gain was also monitored once a week *"data not shown"*.

2.9.2. Sucrose preference test (SPT)

Anhedonia; failure to obtain pleasure from activities previously enjoyed, is a core symptom of MDD. In CMS, anhedonia is measured by calculating the reduction in the consumption of sweet solution or preference as an indicator to the decrease in rewarding properties which is consistent with the failure to obtain pleasure in depressed patients [46].

The discrepancy in the weekly SPT performed for 30 min *"data not show"*; prompted us to experiment a modified 24 h SPT that was not preceded by food and water deprivation [10,47]. Rats were given, for 24 h, a free choice between two 200 ml bottles, one containing tap water and the other containing a 2% sucrose solution, and consumption of water and sucrose solution was calculated by subtracting the weight of the bottles after 24 h and calculated from the following formula [48]:

$$SP = \frac{Sucrose\ intake\ (g)}{Sucrose\ intake\ (g) + Water\ intake\ (g)} \times 100$$

2.9.3. Forced swim test (FST)

FST was performed according to Ref. [49], in order to confirm the ability of the adopted stress paradigm to increase the immobility time, an indicative of depressive behavior. The FST is a 2-day procedure in which rats swim under conditions wherein escape is not possible. Rats were forced to swim in a vertical glass cylinder (diameter 22.5 cm, height 60 cm) containing 35 cm of water maintained at 25 °C. On the

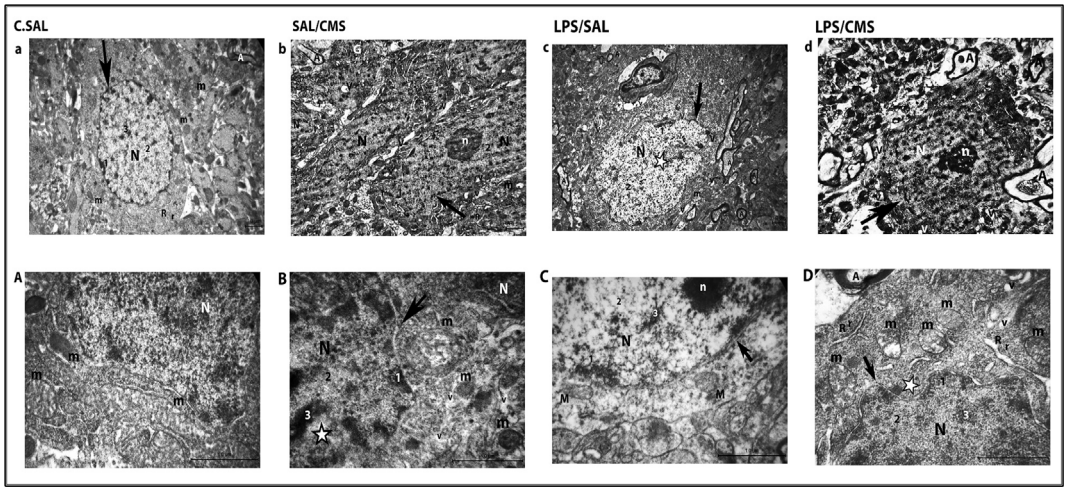

Fig. 3b. Electron micrograph of the hippocampal neurons of rats belonging to the groups: SAL (a, A); SAL/CMS (b, B); LPS/SAL (c, C); LPS/CMS (d, D). In the **SAL group (a)** the nucleus hippocampal neurons (N) shows intact regular nuclear membrane (arrow), peripheral heterochromatine (1), euchromatine (2). The cytoplasm shows cisternae of r ER (R), free ribosomes (r), intact mitochondria (m). With higher magnification **(A)**, mitochondria appear intact with preserved cristae. In the **SAL/CMS (b)** the neuronal nuclei show irregular discontinuous nuclear membrane (arrow), the cytoplasm reveals vacuoles (v), dilated cisternae of r ER (R) and vacuolated mitochondria (m). Higher magnification of neurons of the same group **(B)** shows vacuolated mitochondria with distorted cristae(m) also nuclear membrane forms deep invagination into the nucleus containing part of the cytoplasm(*). Neurons of **LPS/SAL (c)** show also irregularity of the nuclear membrane with deep invagination into the nucleus containing part of the cytoplasm (*), cytoplasmic vacuoles are also seen (V). With higher magnification of neurons of the same group **(C)**, mitochondria of these neurons show some preserved cristae (M). **LPS/CMS (d)** neurons show irregular discontinuous nuclear membrane (arrow) and cytoplasmic vacuoles (v). Higher magnification of neurons of the same group **(D)** shows either vacuolated mitochondria with distorted cristae (m) or mitochondria with preserved cristae (M). The nuclear membrane shows irregularity with deep invaginations into the nucleus containing part of the cytoplasm (*). Also dilated cisternae of rER are seen (R). (Figures a,b,c,d: x8000 and figures A,B,C,D: x30,000).

first day, the rats were trained to swim for 15 min. Water was changed after testing of each animal. Twenty-four hours later, rats were re-exposed to the forced swimming for 5 min. Animal behavior was recorded by a video camera, and immobility time was measured with a stopwatch. The duration of immobility was calculated by summing the total time spent immobile (*viz* the time not spent actively exploring the cylinder or trying to escape from it). Included within the time spent immobile, are the short periods of slight activity where the animals just make those movements necessary to maintain their heads above water [50].

2.9.4. Open-field test (OFT)

The OFT was performed as described by (Blokland et al., 2002) in order to assess the spontaneous locomotion and anxiety-related behaviors in rats. The apparatus consisted of a large black arena 90 × 90 × 60 cm, divided by strips into 25 equal small squares illuminated by white light. Nine central squares were identified as the central zones, while the rest were denoted as the peripheral zones. A Sony USB camera was situated above the arena, such that the entire field was visible. The test was video-taped, and the behavior was subsequently scored by a trained blind observer. A rat was placed in the center of the arena and after 30 s adaptation the number of crossed central and peripheral zones (with at least three paws) were counted manually in a 5 min test. The number of rears (standing upright on the hind paws), the frequency of grooming (including face cleaning, paw licking, fur licking, head scraping and rubbing) and latency to leave the center of the field (inner zone) were also manually calculated during each session [51]. The arena was cleaned by 10% alcohol between trials to eliminate odor cues.

2.10. Transmission electron microscopical examination

Once the animals were anesthetized the chest wall was opened, the sternum was divided in the median plane then the heart was exposed. A Cannula (24 gauge) was inserted in the left ventricle where a mixture of 35 mg heparin in 100 ml saline was infused via the cannula to wash out the blood from the circulation and to avoid the formation of blood clots in the blood vessels of the deep areas of the brain. The right ventricle of the heart was opened to allow blood escape. The fixative (4% gluteraldehyde) was infused through the cannula to allow in situ fixation of deep areas of the brain. Thereafter, animals were decapitated and brains were removed from the skulls. The whole brain was placed in 4% gluteraldehyde for 2 h and then each brain was divided mid-sagitally into right and left hemispheres. Anatomical co-ordinates of the hippocampus were identified [52]. The hippocampi were accessed from the medial sides of the cerebral hemispheres after removal of the whole brain stems and the cerebellums using an inverted scissor. The hippocampi were dissected out from the dorsocaudal aspect of each hemisphere. Small pieces of the hippocampus (1 mm^3) were placed into the gluteraldehyde over night at 4^0c then processed for transmission electron microscopic examination. The hippocampal tissue was postfixed with 1% osmium tetroxide and embedded in epoxy resin. Semi-thin sections were obtained using the ultra-microtome Sumy Electron Optics (SEO, “PEM 100”, Moscow, Russia) and stained with Toluidine Blue and examined with a light microscope. Ultrathin sections were then contrasted with the double stain; uranyl acetate and lead citrate and examined by transmission electron microscope at different magnifications in “The Medical Military Academy”, Cairo, Egypt.

2.11. Statistical analysis

The statistical analyses of the data collected in the behavioral, neurochemical and blood studies were entered, analyzed, and graphically presented using ***“Graphpad Prism, version 5” (***GraphPad software Inc., CA, USA). Normality was assessed by D'Agostino-Pearson normality test. Parametric data were expressed as mean ± SEM and statistical comparisons were carried out using one-way ANOVA followed by Tukey Multiple Comparisons Test. Nonparametric data, < sup > 2 < /sup > data were expressed as median/interquartile range and

[2] For graphical presentation; Bar charts were utilized for parametric data while the Box and whiskers was utilized for non-parametric data.

Table 3
Effects of repeated LPS challenge and CMS protocol either alone or in combination on markers of hippocampal energy metabolism.

Groups	ATP (nmol/mg protein)	ADP (nmol/mg protein)	AMP (nmol/mg protein)	TAN (nmol/mg protein)	AEC	AMP/ATP ratio	p-AMPK (ng/mg protein)
C.SAL (n = 6)	19.72 ± 0.36	4.87 ± 0.21	4.18 ± 0.29	28.43 ± 0.63	0.78 ± 0.00	0.2 ± 0.00	9.53 ± 0.4
SAL/CMS (n = 6)	5.85 ± 0.42 *	14.45 ± 0.07 *	5 ± 0.13 *	25.38 ± 0.8 *	0.51 ± 0.01 *	0.9 ± 0.09 *	92.33 ± 7.81 *
LPS/SAL (n = 6)	5.72 ± 0.38 *	5.9 ± 0.37$^{\#\dagger}$	2.48 ± 0.09 $^{*\#\dagger}$	14.08 ± 0.81 $^{*\#\dagger}$	0.62 ± 0.00 $^{*\#\dagger}$	0.44 ± 0.02 $^{*\#}$	6.91 ± 0.39$^{\#\dagger}$
LPS/CMS (n = 6)	5.68 ± 0.22 *	10.62 ± 0.38 $^{*\#}$	3.52 ± 0.19$^{\#}$	19.74 ± 0.59 $^{*\#}$	0.56 ± 0.01 $^{*\#}$	0.58 ± 0.03 $^{*\#}$	44.11 ± 1.82 $^{*\#}$
ANOVA	$F_{(3,20)}$ = **388.3**, p < **0.0001**	$F_{(3,20)}$ = **99.58**, p < **0.0001**	$F_{(3,20)}$ = **32.15**, p < **0.0001**	$F_{(3,20)}$ = **78.41**, p < **0.0001**	$F_{(3,20)}$ = **312.6**, p < **0.0001**	$F_{(3,20)}$ = **38.93**, p < **0.0001**	$F_{(3,20)}$ = **98.31**, p < **0.0001**

Data are presented as mean ± S.E.M. For comparisons among groups, one-way ANOVA followed by the post hoc "Tukey's Multiple Comparison Test" was utilized. *p < 0.05 significant in comparison to C.SAL, $^{\dagger}p$ < 0.05 significant in comparison to the LPS/CMS, $^{\#}p$ < 0.05 significant in comparison to LPS/CMS-FLX, Ψ p < 0.001 significant in comparison to LPS/CMS-PTX/FLX.
ATP: Adenosine triphosphate; **ADP**: Adenosine diphosphate; **AMP:** Adenosine monophosphate; **TAN**: Total adenine nucleotides; **AEC:** Adenylate energy charge; **p-AMPK:** Phosphorylated AMP activated protein kinase; **C.SAL:** Control saline; **FLX:** Fluoxetine (10 mg/kg i.p); **PTX:** Pentoxiphylline (100 mg/kg i.p); **LPS:** Lipopolysaccharides (50 μg/kg i.p, every other day, a total of six doses); **CMS:** Chronic mild stress (4 weeks).

Table 4
Effects of repeated LPS challenge and CMS protocol either alone or in combination on serum biomarkers.

Groups	CORT (ng/ml)	TNF-α (pg/ml)
C.SAL (n = 6)	31.83 ± 0.7	28.39 ± 0.89
SAL/CMS (n = 6)	235.8 ± 3.85 *	241.9 ± 4.52 *
LPS/SAL (n = 6)	21.85 ± 0.58$^{\#\dagger}$	16.81 ± 0.47$^{\#\dagger}$
LPS/CMS (n = 6)	160.6 ± 3.45 $^{*\#}$	157.9 ± 3.72 $^{*\#}$
ANOVA	$F_{(3,20)}$ = **1561**, p < **0.0001**	$F_{(3,20)}$ = **1278**, p < **0.0001**

Data are presented as mean ± S.E.M. For comparisons among groups, one-way ANOVA followed by the post hoc "Tukey's Multiple Comparison Test" was utilized. *p < 0.001 in comparison to C.SAL, $^{\#}p$ < 0.01 significant in comparison to SAL/CMS and $^{\dagger}p$ < 0.001 significant in comparison to LPS/CMS.
CORT: Corticosterone; **TNF-α:** Tumor necrosis factor alpha; **C.SAL:** Control saline; **LPS:** Lipopolysaccharides (50 μg/kg i.p, every other day, a total of six doses); **CMS:** Chronic mild stress (4 weeks).

Kruskal–Wallis (KW) test was utilized followed by post-hoc Dunn's test. The minimal level of significance was identified at p < 0.05.

3. Results

3.1. Effects of LPS, CMS (separate or combined)

3.1.1. Effects of LPS, CMS (separate or combined) on TLR4 expression and signaling

All the applied exposures; (SAL/CMS, LPS/SAL and LPS/CMS) displayed a significant increase in the expression of TLR4 [$F_{(3,21)}$ = 50.26, p < 0.0001], MyD88 [$F_{(3,21)}$ = 91.38, p < 0.0001], NFκB [$F_{(3,21)}$ = 49.15, p < 0.0001] as well as the level of their downstream player TNF-α [$F_{(3,20)}$ = 538.7, p < 0.0001] as demonstrated in (Fig. 2**).** The SAL/CMS exposure induced a significant increase in the relative expression of TLR4 (11.6 fold), MyD88 (7.38 fold), NFκB (12.89 fold) and the level of hippocampal TNF-α (4.73 fold) in comparison to the control. Similarly, LPS/SAL exposure showed an enhancement in the expression of the aforementioned parameters but with a lower intensity; TLR4 (5.1 fold), MyD88 (6.2 fold), NFκB (4.94 fold). However, hippocampal level of TNF-α showed no significant change in comparison to the control.

Analogously, LPS/CMS combined exposure induced a significant increase in the relative expression of TLR4 (6.06 fold), MyD88 (4.76 fold), NFκB (7.72 fold) and the level of hippocampal TNF-α (2.78 fold) in comparison to the control. Nonetheless, the combined LPS/CMS exposure attenuated the expression of TLR4 (47.8%), MyD88 (32.48%), NFκB (39.4%) as well as the hippocampal level of TNF-α (41.19%), in comparison to SAL/CMS. Simultaneously, LPS/CMS showed a higher expression of NFκB (1.58 fold) and TNF-α level (3.87 fold) as well as a significant decrease in the expression of MyD88 (23.23%) in comparison to LPS/SAL were also observed.

3.1.2. Effects of LPS, CMS (separate or combined) on the expression of mitochondrial biogenesis markers

All the applied exposures; (SAL/CMS, LPS/SAL and LPS/CMS) induced a significant decrease in the expression of PGC1-α [$F_{(3,21)}$ = 82.55, p < 0.0001], NRF1 [$F_{(3,21)}$ = 175.7, p < 0.0001], TFAM [$F_{(3,21)}$ = 155.7, p < 0.0001] and mt-DNA content [$F_{(3,21)}$ = 204.2, p < 0.0001] as demonstrated in (Fig. 3a**).**

SAL/CMS was associated with a significant decrease in the relative expression of PGC1-α (86.92%), NRF1 (80.2%), TFAM (91.1%) as well as a notable decline in mt-DNA content in comparison to the control group. Similarly, the LPS/SAL group showed a significant decline in the expression of PGC1-α (34.58%), NRF1 (14.85%) and TFAM (45.54%) and a significant reduction in mt-DNA content (19.42%) in comparison to the control.

The combined LPS/CMS model showed a notable reduction in the

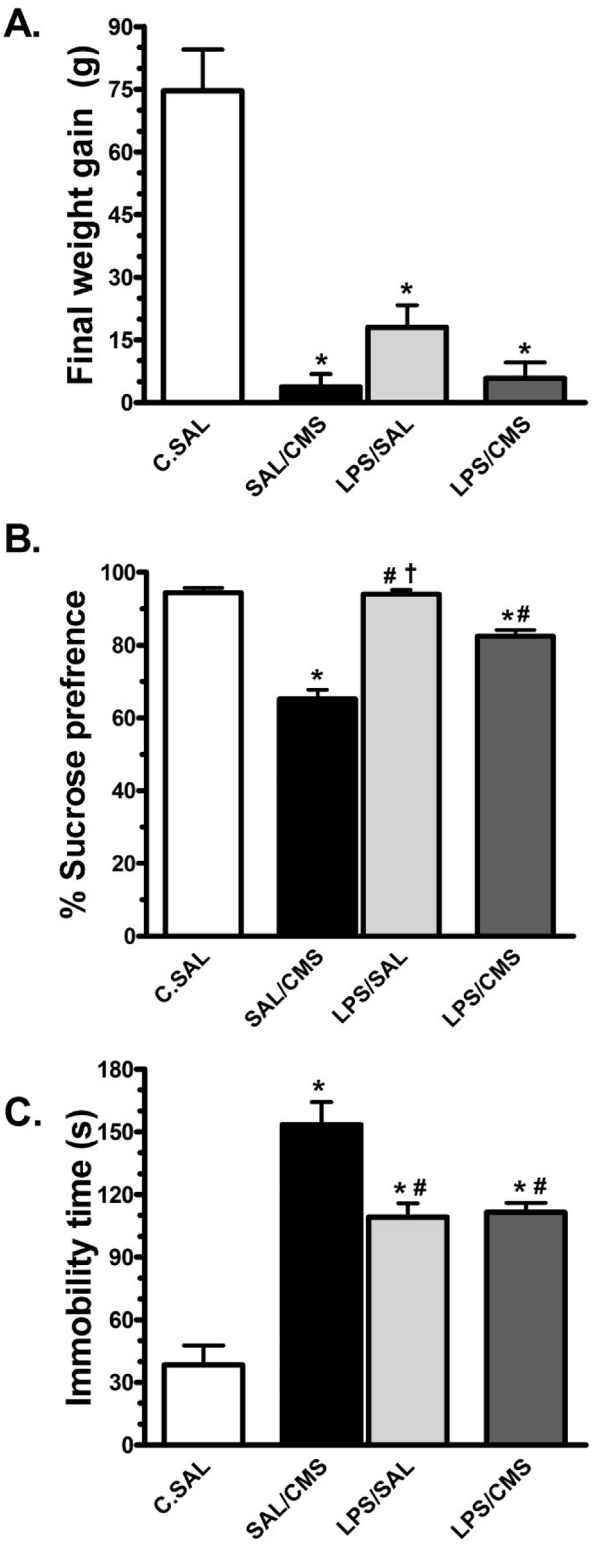

Fig. 4. Effects of LPS, CMS (separate or combined) on weight gain and behavioral changes

Bar graph illustrating changes in (A) Final weight gain; (B) %Sucrose preference; (C) Immobility time in the FST among groups. Data are presented as mean ± S.E.M. C.SAL (n = 11), SAL/CMS (n = 16), LPS/SAL (n = 11) and LPS/CMS (n = 18. For comparisons among groups, one-way ANOVA followed by the post hoc "Tukey's Multiple Comparison Test" was utilized. $^{*}p < 0.001$ significant in comparison to C.SAL, $^{\#}p < 0.01$ significant in comparison to CMS, $^{\dagger}p < 0.001$ significant in comparison to LPS/CMS

C.SAL: Control saline; LPS: Lipopolysaccharides Lipopolysaccharides (50 μg/kg i.p., every other day, a total of six doses); CMS: Chronic mild stress (4 weeks).

relative expression of PGC1-α, NRF1, TFAM and mt-DNA content in comparison to the control (34.58%, 57.43%, 74.26% and 56.31%, respectively). However, it showed a significant higher expression of PGC1-α, NRF1, TFAM as well as the mt-DNA compared to SAL/CMS (2.57, 2.15, 2.89 and 1.88 folds, respectively). However, these values were still significantly lower than those of the C.SAL.

On the other hand, LPS/CMS showed a lower expression of PGC1-α, NRF1, TFAM as well as the mt-DNA content (48.57%, 51.69%, 52.73% and 45.78%, respectively) compared to LPS/SAL.

3.1.3. Effects of LPS, CMS (separate or combined) on the markers of hippocampal energy metabolism

3.1.3.1. Adenine nucleotides and their metabolic ratios. Rats exposed to (SAL/CMS, LPS/SAL and LPS/CMS) showed a significant decline in the concentration of **ATP** in the hippocampal tissue in comparison to the control [70.33%, 70.99% and 71.2%, respectively). Noteworthy, the ATP observed in LPS/CMS were comparable to that scored by the single exposures (SAL/CMS and LPS/SAL). A notable elevation in the **ADP** level was perceived in the SAL/CMS and LPS/CMS groups relative to the control (2.97 and 2.18 folds, respectively). However, the combined LPS/CMS exposure showed a significantly lower ADP level in comparison to SAL/CMS (26.51%) and a higher ADP level in comparison to LPS/SAL (1.8 fold).

Regarding the **AMP** level, SAL/CMS showed a significant increase in the AMP level (1.2 fold), while LPS/SAL showed a significant decrease in the AMP level (40.67%) compared to the control. The AMP level in the combined LPS/CMS exposure was significantly lower than SAL/CMS (29.6%) and comparable to LPS/SAL.

In the present study, all the utilized exposures showed a significant decrease in the hippocampal energy status; manifested via the significant decrease in the **AEC**; SAL/CMS (33.33%), LPS/SAL (20.51%) and LPS/SAL (28.21%) in comparison to the control. However, the single exposure LPS/SAL showed a better energy status; where it's AEC was significantly higher than SAL/CMS (1.22 fold) and LPS/CMS (1.11 fold).

All the applied exposures induced a significant elevation in the **AMP/ATP ratio** in comparison to the control; SAL/CMS (4.5 fold), LPS/SAL (2.2 fold) and LPS/CMS (2.9 fold). These findings are not unexpected, since the major bridge between energy synthesis and energy regulation is the elevation in the AMP/ATP ratio. However, the LPS/CMS group showed a significantly lower AMP/ATP ratio (35.56%) compared to SAL/CMS and a non-significantly higher AMP/ATP ratio (31.82%) in comparison to LPS/SAL.

Accordingly, in the current investigation, the different exposures, either singly or in combination, displayed a significant decline in the hippocampal energy status, manifested as a decrease in AEC paralleled with an increase in the ADP level and AMP/ATP ratio **(**Table 3**).**

3.1.3.2. Activated AMPK (p-AMPK). The observed escalation in the AMP/ATP ratio in (SAL/CMS and LPS/CMS) was paralleled by an increase in the level of p-AMPK by (9.69 and 4.63 folds, respectively) in comparison to the control. However, LPS/SAL didn't show any elevation in the p-AMPK in spite of the significant upsurge in the AMP/ATP ratio **(**Table 3**).** Notably, the combined model LPS/CMS hindered the increase in p-AMPK level by (52.23%) compared to SAL/CMS **(**Table 3**).**

3.1.4. Effects of LPS, CMS; (separate or combined) on serum biomarkers

The single exposure to SAL/CMS induced a significant elevation in the serum levels of CORT and TNF-α in comparison to the control (7.41 and 8.52 folds, respectively). However, LPS/SAL had no effect on the serum level of CORT and TNF-α compared to the control.

The combined LPS/CMS exposure engendered a considerable elevation in the serum level of CORT and TNF-α compared to the control (5.05 and 5.5.6 folds, respectively). Nonetheless, the LPS/CMS-induced elevation in the serum CORT and TNF-α was significantly lower than

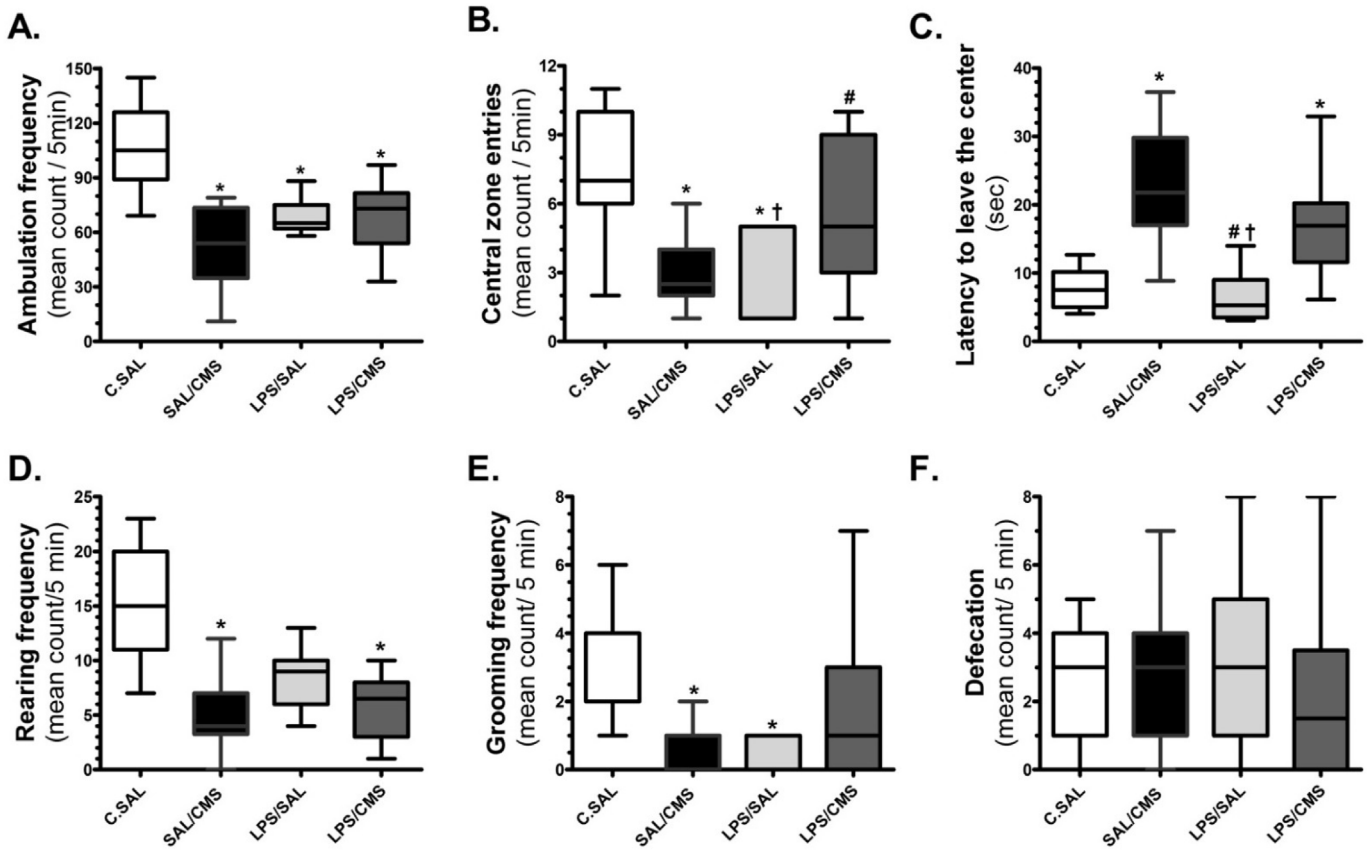

Fig. 5. Effects of different stress exposures on the behavioral changes in open field test
Box-Whisker graph illustrating changes in the OFT in rats exposed to different stressful protocols; **(A)** Central zone entries; **(B)** Total ambulation; **(C)** Latency to leave the center zone; **(D)** Rearing; **(E)** Grooming and **(F)** Defecation. Data are presented as median/interquartile range. C.SAL (n = 11), SAL/CMS (n = 16), LPS/SAL (n = 11) and LPS/CMS (n = 18). For comparisons among groups, Kruskal-Wallis Test followed by post hoc "Dunn's Multiple Comparisons Test" was utilized. $^{*}p < 0.05$ significant in comparison to C.SAL, $^{\#}p < 0.05$ significant in comparison to SAL/CMS, $^{\dagger}p < 0.05$ significant in comparison to the LPS/CMS.
C.SAL: Control saline; **LPS:** Lipopolysaccharides (50 μg/kg i.p., every other day, a total of six doses); **CMS:** Chronic mild stress (4 weeks).

that induced by SAL/CMS (31.89% and 34.73%, respectively). On the other hand, the serum level of CORT and TNF-α in the LPS/CMS group was remarkably higher than that instigated in LPS/SAL group (7.35 and 9.39 folds, respectively) as seen in (Table 4).

3.1.5. Effects of LPS, CMS (separate or combined) on weight gain and behavioral changes

3.1.5.1. Final weight gain. All exposures showed a significant decline in the final body weight gain; SAL/CMS (95.06%), LPS/SAL (75.88%) and LPS/CMS (92.26%) in comparison to the control [$F_{(3,52)} = 34.14$, $p < 0.0001$] as presented in (Fig. 4A). Notably; LPS/CMS didn't show any improvement in the final body weight gain in comparison to the single exposure SAL/CMS.

3.1.5.2. Behavioral tests

3.1.5.2.1. Sucrose preference test (SPT). A significant decline in the final SP was observed in SAL/CMS (27.52%) and LPS/CMS (12.66%) exposures [$F_{(3,52)} = 46.94$, $p < 0.0001$]. However, LPS/SAL didn't induce any changes in the SP as portrayed in (Fig. 4B). Remarkably, LPS/CMS induced a significant escalation in the SP by (26.43%) in comparison to SAL/CMS paralleled with a notable decline (12.29%) in comparison to LPS/SAL (Fig. 4B).

3.1.5.3. Forced swim test. All the applied exposures (SAL/CMS, LPS/SAL and LPS/CMS) displayed a significant increase in the rats' depressive-like behavior [$F_{(3,52)} = 30.96$, $p < 0.0001$], manifested as a significant increase in the immobility time (4, 2.85 and 2.85 folds, respectively) in comparison to the control group (Fig. 4C).

Notably, the depressive behavior scored by the combined LPS/CMS exposures was significantly lower than that scored by SAL/CMS (28.81%). However, the despair behavior scored in the LPS/SAL group was comparable to that scored in LPS/CMS group.

3.1.5.4. Open-field test (OFT). All the employed stressful exposures showed a notable decrease in the **total ambulation** frequency [KWS = 23.81, $p < 0.0001$]. A notable reduction was observed in SAL/CMS (48.57%), LPS/SAL (38.1%) and LPS/CMS (30.48%) groups in comparison to the control (Fig. 5A). However, no significant enhancements were observed when comparing the ambulation frequency of the combined stress model LPS/CMS with the single stress exposures.

Regarding the frequency of **central zone entries** [KWS = 22.96, $p < 0.0001$]; a significant reduction was observed in SAL/CMS and LPS/SAL groups (64.29% and 85.71%, respectively) in comparison to the control group. Although, the frequency of central zone entries scored in LPS/CMS group was significantly lower than that observed in SAL/CMS (50%), yet it was higher than that scored in LPS/SAL (5 folds) as depicted in (Fig. 5B).

Rats exposed to SAL/CMS and LPS/CMS showed a significant increase in the **latency time to leave the central zone** (2.9 and 2.25 folds, respectively) compared to the control group (KWS = 34.21, $p < 0.0001$). The combined stress model LPS/CMS didn't show any significant reduction in the latency time in comparison to SAL/CMS (Fig. 5C). Nonetheless, the latency time to leave the central zones in the LPS/CMS group was significantly higher than that in the LPS/SAL (3.21 fold).

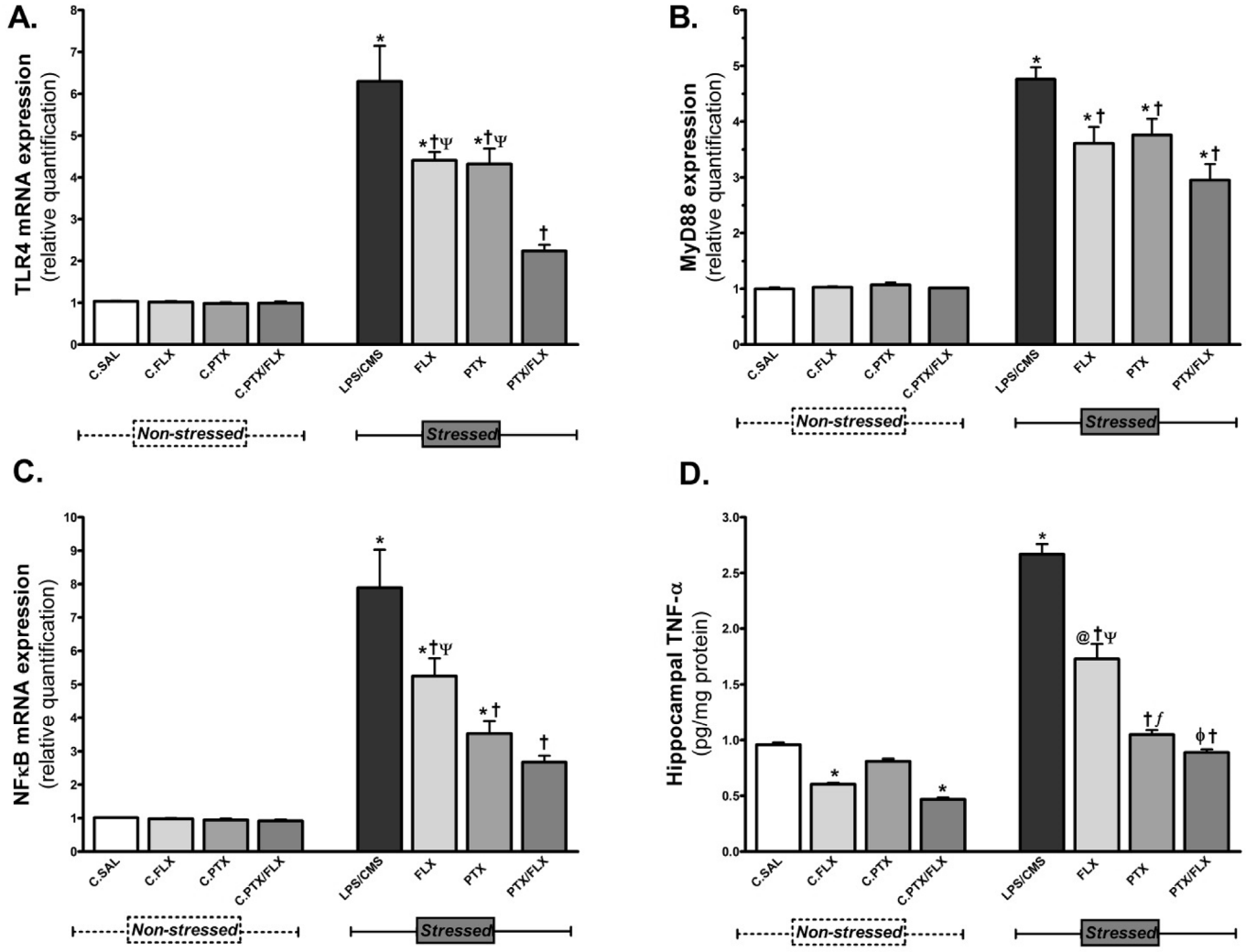

Fig. 6. Effects of FLX and PTX (singly or in combination) on the changes in TLR4 expression and signaling induced by LPS/CMS combined model
Bar graphs illustrating changes in the relative expression of: (A) TLR4, (B) MyD88, (C) NFκB and (D) tTNF-α. Data are presented as mean ± S.E.M. C.SAL (n = 6), C.FLX (n = 6), C.PTX (n = 6), C.PTX/FLX (n = 6), LPS/CMS (n = 7), LPS/CMS-FLX (n = 7), LPS/CMS-PTX (n = 6), LPS/CMS-PTX/FLX (n = 7). For comparisons among groups, one-way ANOVA followed by the post hoc "Tukey's Multiple Comparison Test" was utilized. $^{*}p < 0.05$ significant in comparison to C.SAL, $^{@}p < 0.001$ significant in comparison to C.FLX, $^{\Phi}p < 0.001$ significant in comparison to C.PTX/FLX, $^{\dagger}p < 0.05$ significant in comparison to LPS/CMS, $^{f}p < 0.001$ in comparison to LPS/CMS-FLX, < SUP > Ψ < /SUP > $p < 0.05$ in comparison to LPS/CMS-PTX/FLX.
Non-stressed: control groups not subjected to stress; Stressed: challenged with the combined LPS/CMS model; TLR4: Toll like receptor 4; MyD88: Myeloid differentiation primary response 88; NFκB: Nuclear factor kappa-B; TNF-α: issue tumor necrosis factor α, C.SAL: Control saline; FLX: Fluoxetine (10 mg/kg i.p.); PTX: Pentoxiphylline (100 mg/kg i.p.); LPS: Lipopolysaccharides (50 μg/kg i.p., every other day, a total of six doses); CMS: Chronic mild stress (4 weeks).

A significant decline in the **rearing frequency** was noticed in SAL/CMS and LPS/CMS groups (73.33% and 56.67%, respectively) in comparison to the control group [KWS = 24.3, $p < 0.0001$]. No significant changes were observed when comparing the combined stress model LPS/CMS with the single stressful exposures **(**Fig. 5D**).**

Rats exposed to SAL/CMS and LPS/SAL displayed a significant decrease in the **grooming frequency** by (50% and 100%, respectively) in comparison to the control group (KWS = 19.34, $p = 0.0002$). The combined LPS/CMS exposure didn't show a significant improvement in the grooming frequency compared to the single stressful exposures **(**Fig. 5E**).**

3.1.6. Effects of LPS, CMS (separate or combined) on ultra-structural changes in the hippocampus

Ultra-structural changes of the hippocampal neurons were evaluated by transmission electron microscopy. The hippocampal neurons of C.SAL group were morphologically normal with rounded nuclei that showed a clear and regular double nuclear membrane with peripheral heterochromatine and homogenous euchromatine. The mitochondria and endoplasmic reticulum were intact with abundant ribosomes **(**Fig. 3b **- panels a & A).**

Hippocampal neurons of rats exposed to SAL/CMS, LPS/SAL and LPS/CMS showed signs of neurodegeneration. The nuclei possessed irregular discontinuous nuclear membrane which formed deep invagination into the nucleus containing part of the cytoplasm. The cytoplasm revealed vacuoles, dilated cisternae of rough endoplasmic reticulum. With higher magnification mitochondria of the neurons of SAL/CMS, appeared vacuolated with distorted crista **(**Fig. 3b **- pannels b & B).** In LPS/SAL group the mitochondria showed some preserved cristae **(**Fig. 3b**-pannels c & C).** In LPS/CMS group some mitochondria appeared vacuolated with distorted cristae and others showed preserved cristae **(**Fig. 3b **- pannels d & D).**

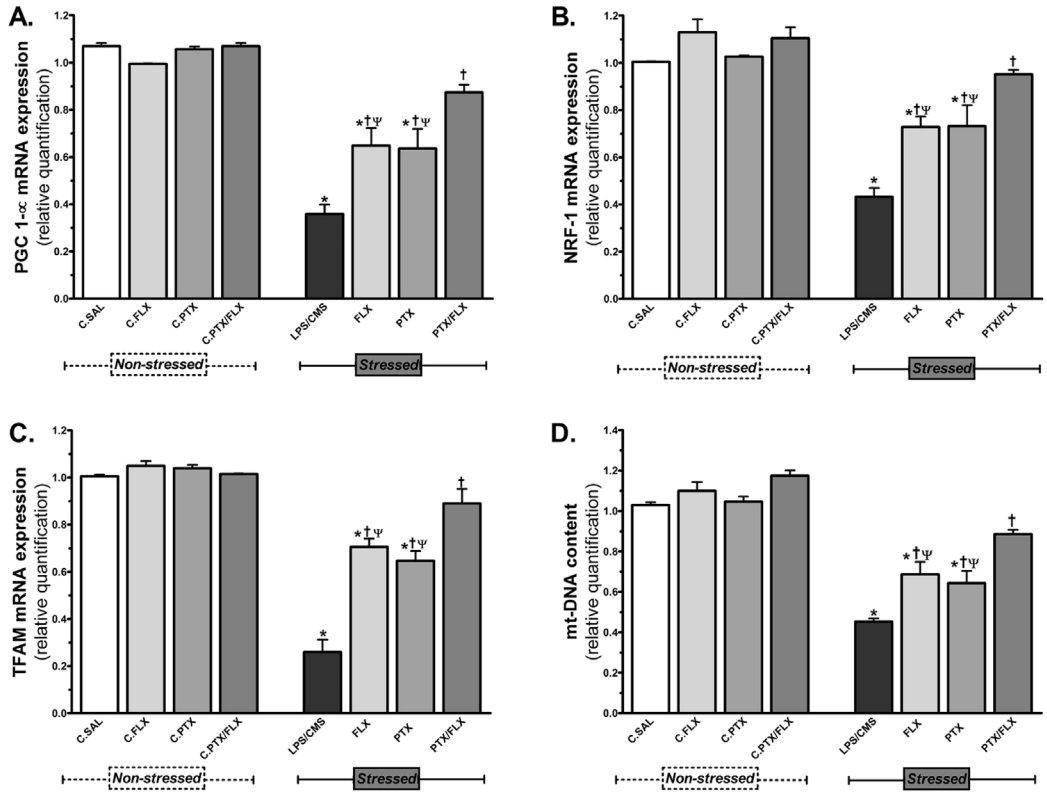

B

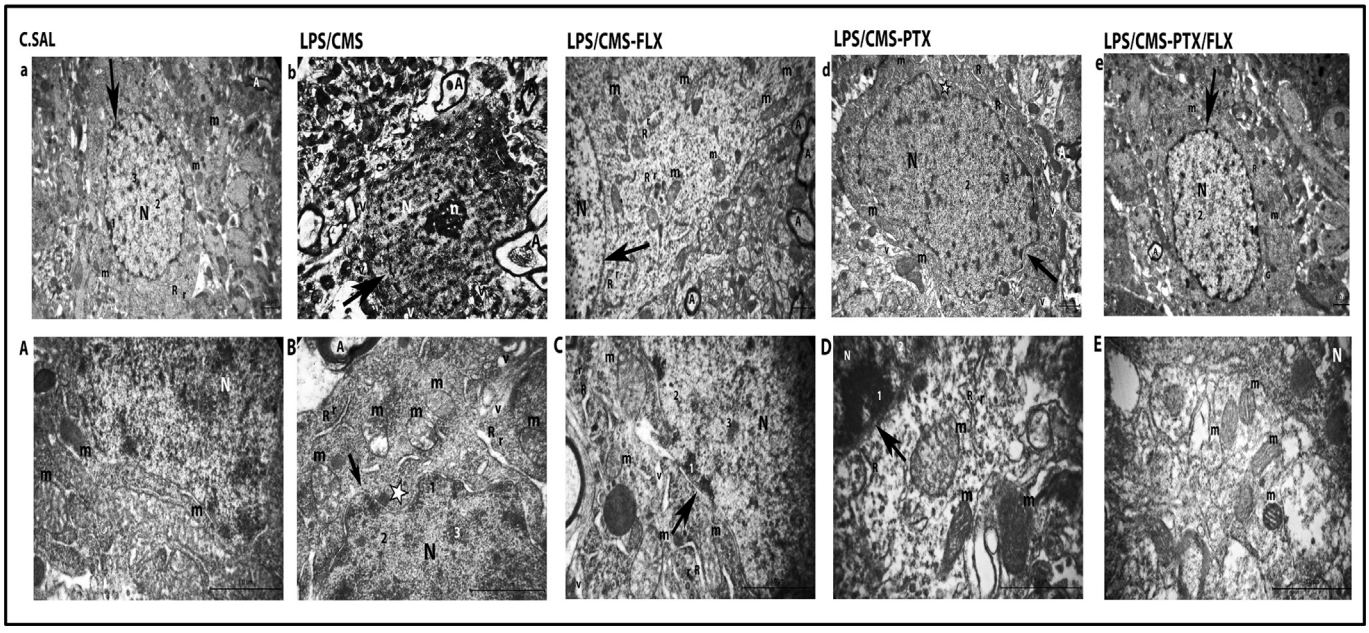

(caption on next page)

3.2. Effects of FLX and PTX (singly or in combination) on changes induced by LPS/CMS combined model

All results are interpreted in comparison to the C.SAL group, unless the positive control groups (C.FLX, C.PTX, C.PTX/FLX) demonstrated a statistically significant difference in comparison to the C.SAL group. The C.SAL and LPS/CMS groups utilized in the previous comparison of the single versus the combined LPS and CMS exposure were further used in this comparative level as well.

3.2.1. Effects of FLX and PTX (singly or in combination) on the changes in TLR4 expression and signaling induced by LPS/CMS combined model

Single treatment with FLX or PTX as well as their combination PTX/FLX ameliorated the LPS/CMS induced enhancement in the relative expression of TLR4 [$F_{(7,\ 43)} = 32.3$, $p < 0.0001$], MyD88 [$F_{(7,\ 43)} = 56.51$, $p < 0.0001$] and NFκB [$F_{(7,43)} = 26.04$, $p < 0.0001$]. Downhill from the aforementioned alterations a consequent modification in the tissue TNF-α level was also observed [$F_{(7,\ 40)} = 142.5$, $p < 0.0001$].

Fig. 7. a: **Effects of FLX and PTX treatment (singly or in combination) on the changes in the expression of mitochondrial biogenesis markers induced by LPS/CMS combined model**.

Bar graphs illustrating changes in the expression of: **(A)** PGC1-α, **(B)** NRF-1, **(C)** TFAM and **(D)** mt-DNA content. Data are presented as mean ± S.E.M. C.SAL (n = 11), C.FLX (n = 9), C.PTX (n = 11), C.PTX/FLX (n = 11), LPS/CMS (n = 18), LPS/CMS-PTX/FLX (n = 18), LPS/SAL-PTX (n = 17), LPS/CMS-PTX/FLX (n = 16). For comparisons among groups, one-way ANOVA followed by the post hoc "Tukey's Multiple Comparison Test" was utilized. *$p < 0.01$ significant in comparison to C.SAL, $^{\dagger}p < 0.05$ significant in comparison to LPS/CMS, $^{@}p < 0.05$ in comparison to C.FLX and < SUP > Ψ < /SUP > $p < 0.05$ in comparison to the LPS/CMS-PTX/FLX.

Non-stressed: control groups not subjected to stress; **Stressed:** Challenged with the combined LPS/CMS model; **PGC1- α**: Peroxisome proliferator-activated receptor gamma co-activators 1 **α; NRF-1:** Nuclear respiratory factor 1; **TFAM:** Mitochondrial transcription factor A; **mt-DNA:** Mitochondrial DNA; **C.SAL:** Control saline; **FLX:** Fluoxetine (10 mg/kg i.p); **PTX:** Pentoxiphylline (100 mg/kg i.p); **LPS:** Lipopolysaccharides (50 μg/kg i.p, every other day, a total of six doses); **CMS:** Chronic mild stress (4 weeks).

b**: Electron micrograph of the hippocampal neurons of rats belonging to the groups; C.SAL (a, A); SAL/CMS (b, B); LPS/CMS-FLX (c,C); LPS/CMS-PTX (d,D) and LPS/CMS-PTX-FLX (e,E).**

A normal structure of hippocampal neurons is observed. The nuclear membrane appears regular (arrow). Higher magnification shows normal mitochondria with preserved cristae (m). (Figures a,b,c,d: x8000 and figures A,B,C,D: x30,000).

TLR4 expression was successfully attenuated by FLX, PTX as well as their combination PTX/FLX in comparison to LPS/CMS exposure (30.16%, 31.43%, and 64.44%, respectively). However, the values of both single treatments, FLX and PTX were still significantly higher than the C.SAL (4.23 and 4.15 folds, respectively). The combined treatment PTX/FLX showed a higher attenuation in the expression of TLR4 in comparison to FLX (34.28%) and PTX (33.01%) single treatments that was comparable to the C.SAL **(**Fig. 6A**).**

The down regulation observed in the expression of TLR4 was associated with an analogous decline in the expression of its adaptor protein MyD88; FLX (24.16%), PTX (21.01%) and PTX/FLX (38.03%) as portrayed in **(**Fig. 6B**).** Nonetheless, these values were still significantly higher than C.SAL (3.61, 3.76 and 2.95, respectively). Although the combined treatment PTX/FLX showed a higher attenuation in the MyD88 expression yet this difference was statistically non-significant.

Single treatment with FLX, PTX as well as their combination PTX/FLX significantly decreased the relative expression of NFκB compared to LPS/CMS [33.46%, 55.26%, and 66.16%, respectively). However, the values of both single treatments, FLX and PTX were still significantly higher than the C.SAL (5.2 and 3.5 folds, respectively) **(**Fig. 6C**).** The combined treatment PTX/FLX showed a further reduction in the expression of the NFκB mRNA by (32.7%) in comparison to the FLX-treated group and a non-significant diminution by (10.9%) in comparison to the PTX-treated group. Notably the combined treatment PTX/FLX almost normalized the NFκB expression compared to C.SAL.

Consequently, the single treatment with FLX, PTX and their combination PTX/FLX showed a considerable decrease in the level of their downstream player hippocampal TNF-α (35.21%, 60.67% and 66.67%, respectively) in comparison to LPS/CMS exposure. The combined treatment PTX/FLX showed a notable boost in the retardation of the expression of TNF-α mRNA by (31.46%) in comparison to FLX-treated rats and a non-significant improvement in comparison to the PTX-treated group **(**Fig. 6D**).**

3.2.2. Effects of FLX and PTX treatment (singly or in combination) on the changes in the expression of mitochondrial biogenesis markers induced by LPS/CMS combined model

Single treatment with FLX, PTX as well as their combination PTX/FLX restored the expression of PGC1-α mRNA by (1.81, 1.78 and 2.42 folds, respectively) in comparison to LPS/CMS exposure [$F_{(7, 43)} = 34.73$, $p < 0.0001$]. However, the repair induced by the single treatments FLX and PTX was still significantly lower than C.SAL (39.25% and 40.19%, respectively). Remarkably; the combined treatment PTX/FLX boosted PGC1-α expression to be comparable to that of the C.SAL and significantly higher than that induced by either FLX (33.85%) or PTX (35.94%) treatments alone as depicted in **(**Fig. 7A**).**

Subsequently a significant restoration in the expression of the nuclear transcriptional factor NRF1 was also observed with FLX (1.7 fold), PTX (1.7 fold) as well as their combination PTX/FLX (2.21 fold) in comparison to LPS/CMS. However, the repair induced by the single treatments FLX and PTX was still lower than the C.SAL (27.72% and 27.72%, respectively). Yet, the mending observed with the single treatments FLX and PTX was still significantly lower than C.SAL (29.71% and 35.64%, respectively). Nonetheless, the combined treatment PTX/FLX strengthened this enhancement and restored the expression of NRF1 to be comparable to that of C.SAL and significantly higher than FLX (30.14%) and PTX (30.14%) single treatments [$F_{(7, 43)} = 29.53$, $p < 0.0001$] as demonstrated in **(**Fig. 7B**).**

Single treatment with FLX and PTX as well as their combination PTX/FLX induced a significant enhancement in the expression of the mitochondrial transcription factor TFAM (2.73, 2.5, and 3.42 folds, respectively) in comparison to LPS/CMS. However, the combined treatment PTX/FLX showed a further improvement in the expression of TFAM mRNA comparable to that observed in the C.SAL group and notably higher than FLX (25.35%) and PTX (36.92%) single treatments [$F_{(7, 43)} = 54.57$, $p < 0.0001$] as shown in **(**Fig. 7C**).**

Mitochondrial biogenesis; mediated via both nuclear (NRF1) and mitochondrial transcriptional factors (TFAM) was assessed via the detection of the increase in mt-DNA content. Notably FLX, PTX as well as their combination PX/FLX induced a significant increase in the hippocampal mt-DNA content by (1.53, 1.42 and 1.98 folds, respectively) compared to LPS/CMS [$F_{(7, 43)} = 45.6$, $p < 0.0001$]. However, the repair induced by the single treatments FLX and PTX was still lower than the C.SAL (33.01% and 37.86%, respectively). Remarkably, the combined treatment PTX/FLX showed a further enrichment in the mt-DNA content that was comparable to C.SAL and higher than the content observed with the single treatments FLX and PTX (28.99% and 39.06%, respectively) as shown in **(**Fig. 7D**).**

3.2.3. Effects of FLX and PTX treatment (singly or in combination) on the changes in the markers of hippocampal energy metabolism induced by LPS/CMS combined model

3.2.3.1. Adenine nucleotides and their metabolic ratios. Single treatment with FLX induced a significant rise in the ATP level (1.29 fold) in comparison to LPS/CMS exposure. However, the elevation in the ATP level induced by PTX and PTX/FLX was statistically non-significant (Table 5). The differences among the studied groups were statistically significant as calculated by One-way ANOVA [$F_{(7, 40)} = 623.1$, $p < 0.0001$].

Single treatment with FLX and PTX as well as their combination PTX/FLX showed a notable decline in the ADP level compared to combined LPS/CMS model (12.24%, 29.57% and 38.61%, respectively) as demonstrated in **(**Table 5**).**

Simultaneously, a significant decline in the AMP/ATP ratio was attained in rats receiving a single treatment with FLX, PTX as well as their combination PTX/FLX (22.41%, 36.21% and 25.86%, respectively) in comparison to the combined model LPS/CMS **(**Table 5**).**

A significant enhancement of AEC was demonstrated in rats treated with FLX, PTX and PTX/FLX in comparison to the combined LPS/CMS

Table 5
Effects of FLX and PTX treatment (separate or combined) on the changes induced by LPS/CMS combined model in the adenine nucleotides and their metabolic ratios.

Groups	ATP (nmol/mg protein)	ADP (nmol/mg protein)	AMP (nmol/mg protein)	TAN (nmol/mg protein)	AEC	AMP/ATP ratio	p-AMPK (ng/mg protein)
C.SAL (n = 6)	19.72 ± 0.36	4.87 ± 0.21	4.18 ± 0.29	28.43 ± 0.63	0.78 ± 0.00	0.2 ± 0.00	9.53 ± 0.4
C.FLX (n = 6)	18.7 ± 0.25	4.98 ± 0.02	3.7 ± 0.18	18.7 ± 0.25	0.77 ± 0.01	0.2 ± 0.01	8.36 ± 0.4
C.PTX (n = 6)	18.39 ± 0.18	5.44 ± 0.28	4 ± 0.2	18.39 ± 0.18	0.77 ± 0.00	0.2 ± 0.01	7.65 ± 0.26
C.PTX/FLX (n = 6)	18.39 ± 0.25	5.05 ± 0.07	4.28 ± 0.08	18.39 ± 0.25	0.77 ± 0.00	0.22 ± 0.00	7.1 ± 0.31
LPS/CMS (n = 6)	5.68 ± 0.22 *	10.62 ± 0.38 *	3.52 ± 0.19	19.74 ± 0.59 *	0.56 ± 0.01 *	0.58 ± 0.03 *	44.11 ± 1.82 *
LPS/CMS-FLX (n = 6)	7.3 ± 0.09 *†	8.9 ± 0.3 *† < SUP > Ψ < /SUP >	3.27 ± 0.09 *	19.74 ± 0.42 * < SUP > Ψ < /SUP >	0.6 ± 0.00 *†	0.45 ± 0.01 *†	22.16 ± 0.96 *† < SUP > Ψ < /SUP >
LPS/CMS-PTX (n = 6)	6.58 ± 0.4 *	7.48 ± 0.44 *†f	2.4 ± 0.1 *†f	16.46 ± 0.66 *†f	0.63 ± 0.01 *†	0.37 ± 0.01 *†f	33.5 ± 1.38 *†f < SUP > Ψ < /SUP >
LPS/CMS-PTX/FLX (n = 6)	6.18 ± 0.2 *	6.52 ± 0.37 *†	2.6 ± 0.11 *†	15.31 ± 0.38 *†	0.62 ± 0.08 *†	0.43 ± 0.02 *†	13.94 ± 0.62 *†
ANOVA	$F_{(7,40)} = 623.1, p < 0.0001$	$F_{(7,40)} = 52.03, p < 0.0001$	$F_{(7,40)} = 16.78, p < 0.0001$	$F_{(7,40)} = 149.1, p < 0.0001$	$F_{(7,40)} = 309.8, p < 0.0001$	$F_{(7,40)} = 95.93, p < 0.0001$	$F_{(7,40)} = 219.4, p < 0.0001$

Data are presented as mean ± S.E.M. For comparisons among groups, one-way ANOVA followed by the post hoc "Tukey's Multiple Comparison Test" was utilized. *$p < 0.05$ significant in comparison to C.SAL, †$p < 0.05$ significant in comparison to the LPS/CMS, f$p < 0.05$ significant in comparison to LPS/CMS-FLX, Ψ $p < 0.001$ significant in comparison to LPS/CMS-PTX/FLX.
ATP: Adenosine triphosphate; **ADP**: Adenosine diphosphate; **AMP:** Adenosine monophosphate; **TAN**: Total adenine nucleotides *TAN = (ATP + ADP + AMP)*; AEC: Adenylate energy charge *"AEC = (ATP + 0.5 ADP)/TAN"*; *p*-**AMPK:** Phosphorylated AMP activated protein kinase; **C.SAL:** Control saline; **FLX:** Fluoxetine (10 mg/kg i.p); **PTX:** Pentoxiphylline (100 mg/kg i.p); **LPS:** Lipopolysaccharides (50 μg/kg i.p, every other day, a total of six doses); **CMS:** Chronic mild stress (4 weeks).

model (1.07, 1.13 and 1.11 folds, respectively) as depicted in (Table 5).

Hence, all the applied treatments to the LPS/CMS combined model induced considerable improvement in the hippocampal energy status; manifested via the decline in the ADP, AMP/ATP and the elevation in the AEC.

3.2.3.2. Activated AMPK (p-AMPK). The observed decline in the AMP/ATP ratio in rats treated with FLX, PTX and their combination PTX/FLX, was accompanied by a comparable reduction in the level of p-AMPK in comparison to the LPS/CMS group (49.76%, 24.05% and 68.4%, respectively) (Table 5). The combined treatment PTX/FLX induced a significant further decline in comparison to both FLX and PTX single treatments (37.09% and 58.39%, respectively).

3.2.4. Effects of FLX and PTX treatment (either alone or in combination) on the changes in serum biomarkers induced by LPS/CMS combined model

One-way ANOVA revealed a profound difference between the C.SAL group and the positive control groups. Precisely, the serum levels of CORT and TNF- α were significantly lower in the C.FLX (34.28% and 41.04%, respectively) and C.PTX/FLX (47.47% and 57.2%, respectively) in comparison to the C.SAL. Thus the FLX treated group and PTX/FLX treated group will be compared to their positive control group rather than the C.SAL.

Chronic treatment with FLX, PTX as well as their combination PTX/FLX, successfully ameliorated the LPS/CMS induced elevation in the serum level of CORT (28.64%, 20.05% and 43.8%, respectively) and TNF-α (30.15%, 26.35% and 44.83%, respectively) as described in (Table 6).

Remarkably, the combined treatment (PTX/FLX) induced a better cut off in both biomarkers compared to the single treatments. In particular rats treated with PTX/FLX showed a significantly lower serum CORT level in comparison to the single treatment with FLX (21.25%) or PTX (29.71%). By the same token the serum level of TNF-α in the PTX/FLX-treated group was remarkably lower than that in the singly treated groups with either FLX (21.02%) or PTX (25.09%).

3.2.5. Effects of FLX and PTX treatment (singly or in combination) on the changes in weight gain and behavior induced by LPS/CMS combined model

3.2.5.1. Final body weight gain. One-way ANOVA revealed a significant difference between the C.SAL group and the positive control groups. (70.89%) In particular C.FLX and C.PTX/FLX showed a significantly lower final weight gain in comparison to C.SAL (70.89% and 8.79%, respectively). Thus the FLX treated group and PTX/FLX treated group will be compared to their positive control group rather than the C.SAL.

Rats treated with FLX a classical AD known to induce weight loss, showed a significant reduction in the body weight gain in comparison to the LPS/CMS group (793.9%). Noteworthy, FLX treatment showed a drastic reduction in the body weight gain even in comparison to the C.FLX group by (284.58%). This paradoxical decrease in body weight gain upon treatment with FLX may be attributed to the notion that enhancement of the serotonergic system, alters food intake both quantitatively and qualitatively and decrease the leptin level even in the absence of stress exposure (Gamaro et al., 2008). On the other hand, PTX treatment prompted a significant escalation in the final body weight gain (3.93 fold) in comparison to the LPS/CMS (Fig. 8A).

However, the combined PTX/FLX treatment exhibited a non-significant improvement in the body weight gain in comparison to the LPS/CMS group. The differences among the studied groups were statistically significant as calculated by One-way ANOVA [F (7, 103) = 35.88, $p < 0.0001$].

3.2.5.2. Behavioral changes

3.2.5.2.1. Final sucrose preference test. FLX, PTX and their combination PTX/FLX failed to restore the decline in the SP induced by the combined LPS/CMS model [$F_{(7,\ 103)} = 7.67$, $p < 0.0001$]. Paradoxically the FLX and PTX/FLX treated rats showed a

Table 6
Effects of FLX and PTX treatment either alone or in combination on serum biomarkers in rats exposed to the combined stress model LPS/CMS.

Groups	CORT (ng/ml)	TNF-α (pg/ml)
C.SAL (n = 6)	31.83 ± 0.7	28.39 ± 0.89
C.FLX (n = 6)	20.92 ± 0.55 *	16.74 ± 0.9 *
C.PTX (n = 6)	26.08 ± 0.41	20.59 ± 0.53
C.PTX/FLX (n = 6)	16.72 ± 0.44 *	12.15 ± 0.4 *
LPS/CMS (n = 6)	160.6 ± 3.45 *	157.9 ± 3.72 *
LPS/CMS-FLX (n = 6)	114.6 ± 1.43 $^{@\dagger}$ < SUP > Ψ < /SUP >	110.3 ± 1.64 $^{@\dagger}$ < SUP > Ψ < /SUP >
LPS/CMS-PTX (n = 6)	128.4 ± 1.02 $^{*\dagger f}$ < SUP > Ψ < /SUP >	116.3 ± 2.69 $^{*\dagger f}$ < SUP > Ψ < /SUP >
LPS/CMS-PTX/FLX (n = 6)	90.25 ± 2.45 $^{\Phi\dagger}$	87.12 ± 2.44 $^{\Phi\dagger}$
ANOVA	**$F_{(7,40)}$ = 1165, p < 0.0001**	**$F_{(7,40)}$ = 1073, p < 0.0001**

Data are presented as mean ± S.E.M. For comparisons among groups, one-way ANOVA followed by the post hoc "Tukey's Multiple Comparison Test" was utilized. *p < 0.001 significant in comparison to C.SAL, $^{@}p$ < 0.001 significant in comparison to C.FLX, ϕp < 0.001 significant in comparison to C.PTX/FLX, $^{\dagger}p$ < 0.001 significant in comparison to LPS/CMS, ^{f}p < 0.001 significant in comparison to LPS/CMS-FLX and Ψp < 0.001 significant in comparison to LPS/CMS-PTX/FLX.

CORT: Corticosterone; **TNF-α:** Tumor necrosis factor α; **C.SAL:** Control saline; **FLX:** Fluoxetine (10 mg/kg i.p); **PTX:** Pentoxiphylline (100 mg/kg i.p); **LPS:** Lipopolysaccharides (50 μg/kg i.p, every other day, a total of six doses); **CMS:** Chronic mild stress (4 weeks).

significantly lower SP in comparison to C.SAL (11.6% and 8.78%). In spite of this, their SP was still comparable to that of the corresponding positive control groups (C.FLX and C.PTX/FLX group). Although the SP of the PTX treated group was comparable to that of the C.SAL group; yet statistically it was not significant from the LPS/CMS group **(**Fig. 8B**).**

3.2.5.3. Forced swim test. In the FST the immobile behavior is usually interpreted as a measure of depressive-like behavior which could be further reduced by AD treatment (Porsolt et al., 1977). As anticipated, rats treated with the classical AD "FLX" induced a significant reduction in the immobility time by (36.46%) in comparison to LPS/CMS group. Interestingly, challenging the cytokine theory of depression; PTX treatment; an anti-TNF-α drug induced a significant reduction in the immobile behavior by (33.9%) in comparison to LPS/CMS group. Even though, both single treatments induced a comparable decline in the immobile behavior, yet only FLX treated rats we almost approaching the C.SAL group **(**Fig. 8C**).**

The combined treatment PTX/FLX induced a further decline in the immobility time in comparison to LPS/CMS (47.8%). Notably, the immobility time scored in the PTX/FLX treated rats was comparable to that of C.SAL. However, this enhanced diminution was statistically non-significant compared to the single treatments. The differences among the studied groups were statistically significant as calculated by One-way ANOVA [$F_{(7,\ 103)}$ = 10.91, p < 0.0001].

3.2.5.4. Open-field test. A notable change in the ambulation frequency, latency to leave the central zone and the rearing frequency was attained upon treating the animals exposed to the combined stress model LPS/CMS with PTX, FLX or their combination PTX/FLX **(**Fig. 9**).** Nevertheless, statistical analysis revealed no significant difference among the treated groups, the LPS/CMS exposure and the controls; regarding the frequencies of central zone entries, grooming and defecation frequencies. The differences among the studied groups were statistically significant as calculated by Kruskal-Wallis nonparametric test for the different behaviors scored in the OFT; (i) ambulation frequency [KWS = 30.43, p < 0.0001], (ii) Central zone entries [KWS = 6.37, p = 0.497], (iii) latency to leave the central zone [KWS = 6.37, p = 0.497] (iv)rearing [KWS = 36.55, p < 0.0001], (iv) grooming frequency [KWS = 13.93, p = 0.0524] and (v) defecation frequency [KWS = 5.14, p = 0.6425].

FLX treatment induced a significant decrease in the LPS/CMS-induced anxiogenic behavior apprehended from the notable 48.97% decline in the latency time to leave the central zone compared to the LPS/CMS group (Fig. 9b). Moreover, rats treated with FLX demonstrated an enhanced locomotor activity; manifested through the significant 100% elevation in the rearing frequency "vertical locomotor activity" compared to the LPS/CMS group (Fig. 9C). However, FLX treatment didn't show any significant improvement in the ambulation frequency and central zones entries.

Regarding the PTX treatment, it only showed an improvement in the rearing frequency (2.15 fold) compared to the LPS/CMS exposure **(**Fig. 9C**).** Although the PTX-treated rats showed a statistically insignificant decrease in the latency time in comparison to the LPS/CMS by (10.03%), yet the scored latency time was statistically insignificant from that scored in the C-PTX group and significantly higher than that of C-SAL group (2.03 fold). Notably; the latency time in the C.PTX group was significantly higher than the C.SAL, while the C.FLX and the C.PTX/FLX were non-significantly different from the C.SAL. Thus, pointing out to the impact of PTX administration on the latency time even in the absence of any stressful stimuli.

Rats treated with the combination PTX/FLX demonstrated a significant increase in the rearing frequency (1.69 fold) (Fig. 9C) and a significant lowering of the latency to leave the central zone (44.54%) **(**Fig. 9B**)** compared to LPS/CMS.

3.2.6. Effects of FLX and PTX treatment (either alone or in combination) on the changes in the hippocampus ultra-structure induced by LPS/CMS combined model

Administration of PTX, FLX and their combination to animal exposed to LPS/CMS model showed an improvement of the neurodegenerative changes of hippocampal neurons. In such neurons the nuclear membrane appeared regular and intact with fewer vacuolization in the cytoplasm. At a higher magnification the mitochondria displayed a noticeable structural improvement elucidated via the apparent intact mitochondria with preserved cristae **(**Fig. 7b**).**

4. Discussion

This study highlights the multifaceted communication between the immune, neural and endocrine systems particularly on the sequels of stress-induced dysregulation in any/all of these systems on mitochondrial resilience capacity and hippocampal energy metabolism.

Interestingly, this report associated repeated challenge with low dose LPS to be attenuating, rather than priming, the subsequent CMS responses compared to the study of Elgarf et al. [25]. Such finding supports the concept that environmental factors, such as day-night variations and endogenous rhythms, can also affect immune function and sickness behavior expression [53–59].

The LPS/CMS showed a typical depressive profile (OFT and SPT) and physiological indices (CORT and weight gain) comparable to the well validated CMS model, confirming the face validity of the adopted combined LPS/CMS model [60]. In fact, multiple experimental evidences have documented the occurrence of theses behavioral changes with either manipulation (LPS or CMS) when applied separately. In this

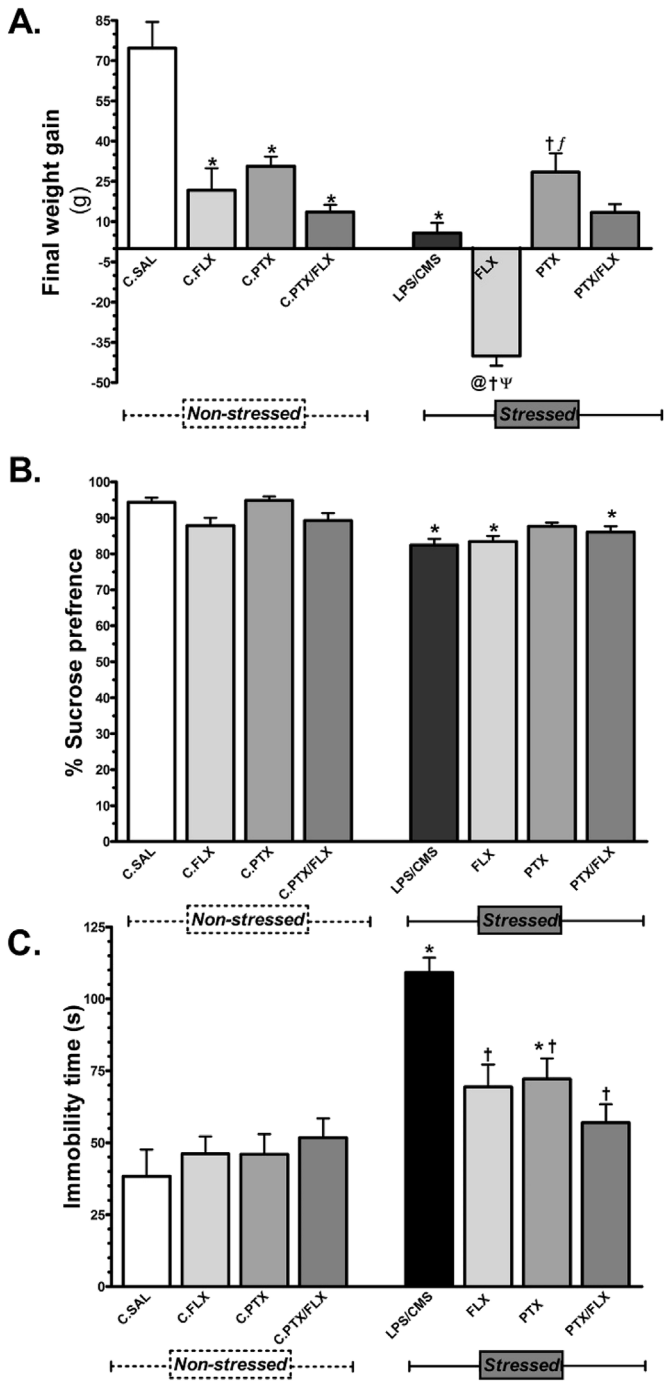

Fig. 8. Effects of FLX and PTX treatment either alone or in combination on the behavioral examination of rats exposed to the combined stress model LPS/CMS.

Bar graphs illustrating changes in: **(A)** Final weight gain; **(B)** 24-hr SPT**; (C)** FST. Data are presented as mean ± S.E.M. C.SAL (n = 11), C.FLX (n = 9), C.PTX (n = 11), C.PTX/FLX (n = 11), LPS/CMS (n = 18), LPS/SAL-FLX (n = 18), LPS/SAL-PTX (n = 17), LPS/SAL-PTX/FLX (n = 16). For comparisons among groups, one-way ANOVA followed by the post hoc "Tukey's Multiple Comparison Test" was utilized. *$p < 0.05$ significant in comparison to C.SAL, $^{@}p < 0.001$ significant in comparison to C.FLX, $^{\dagger}p < 0.05$ significant in comparison to the LPS/CMS, ^{f} $p < 0.001$ in comparison to LPS/CMS-FLX, < SUP > Ψ < /SUP > $p < 0.001$ in comparison to LPS/CMS-PTX/FLX.**Non-stressed:** Control groups not subjected to stress; **Stressed:** Challenged with the combined LPS/CMS model; **C.SAL:** Control saline; **FLX:** Fluoxetine (10 mg/kg i.p.); **PTX:** Pentoxiphylline (100 mg/kg i.p); **LPS:** Lipopolysaccharides (50 μg/kg i.p., every other day, a total of six doses); **CMS:** Chronic mild stress (4 weeks).

line several studies in our lab and in others, reported the association of CMS with the anhedonic behavior (decreased SP) [11,25,36,48,61–63], decrease in locomotor activity (horizontal and vertical) [36,61,64,65] as well as the increase in the anxious behavior in the OFT [66] and desperate behavior in the FST [11,25,60]. Chronic administration of FLX, PTX and their combination, successfully attenuated the LPS/CMS induced elevation in the despair behavior observed in the FST, the anxious behavior in the OFT and the elevated serum CORT. However neither single treatments (FlX or PTX) nor their combination was capable to improve the LPS/CMS induced decline in the SP.

TLRs expression is not static, but rather, modulated by pathogens, cytokines, and environmental stresses [67,68]. In essence, animals exposed to LPS/CMS showed an enhanced expression of TLR4 and its signaling cascade. A plausible explanation for such increment may be attributed to the stress-induced translocation of intestinal endotoxin "leaky gut" [29,69]. A further evidence supporting the role of TLR4 in mediating stress-induced neuroimmune/inflammatory interaction was the observation that TLR4-deficient mice show lower inflammatory response in the brain and a better behavioral outcome in response to immobilization stress [70].

The activation of TLR4 triggers pro-inflammatory transcription *via* its adaptor protein MyD88 which culminates in the activation of the transcriptional factor NFκB, all of which enhancing the production of PICs such as TNF-α [71,72]. In the present study, the enhanced expression of TLR4 was associated by an augmented expression of MyD88, NFκB, and tissue TNF-α (Figs. 2 and 6); findings that are in harmony with previous studies highlighting the role of TLR4 and its downstream players in triggering stress-induced cellular and behavioral changes [73,74] in experimental animals [4,70,75] and in clinical trials [30,31]. FLX treatment decreased the expression of TLR4, NFκB and TNF-α content compared to LPS/CMS, suggesting a potential anti-inflammatory activity of FLX **(**Fig. 6**).** A plausible explanation provided by Lim et al. [76] emphasized the protective effect of FLX in the delayed damaging processes activated in the post ischemic brain *via* suppression of NFκB activity and attenuation of TNF-α in post ischemic brain after reperfusion. PTX, a methylxanthine derivative used for its hemorheological properties, has proved to inhibit transcription of TNF-α [77,78]. Former studies from our lab documented the protective effect of prior treatment with PTX in both CMS [36] alone and in LPS/CMS combined model [25]. Indeed, in the present investigation, PTX provided a comparable anti-inflammatory effect to that of FLX in LPS/CMS protocol manifested as a reduction of the expression of TLR4, MyD88, NFκB and TNF-α level **(**Fig. 6**).** The aforementioned reductions were associated with attenuation in the CORT levels observed in the PTX-treated group in comparison to both SAL/CMS and LPS/CMS groups in line with previous studies done in our lab on CMS [36] and the combined LP/CMS model [25].

PTX/FLX exerted a synergistic neuroprotection compared to LPS/CMS suggesting that the neuroprotection against CMS could be achieved by diverse approaches that taper PICs functioning. This finding is in accordance with a previous clinical study done by our lab testing the efficacy of adding PTX regimen to escitalopram in depressed geriatric patients *(data not published).* In the aforementioned study, it was observed that the need to escalate the dose of escitalopram, was more frequent in the placebo group than in the group receiving PTX. Also, the number of patients achieving remission, compared to responders, after 3 months follow-up, was higher in the PTX group. Thus, the study helped as a proof-of-concept adding to our reported lab workups, advocating its usefulness as an add-on therapy to other antidepressants, especially against inflammatory cytokines induced depression; hence reducing resistance to antidepressants.

Multiple studies delegate the intersection of inflammatory responses and mitochondrial biogenesis as an important mechanism for mediating neuronal neuroprotection against variable stressful stimuli [17,79–81]. Such finding supports the notion that stress-induced post inflammatory induction of mitochondrial quality control processes, particularly

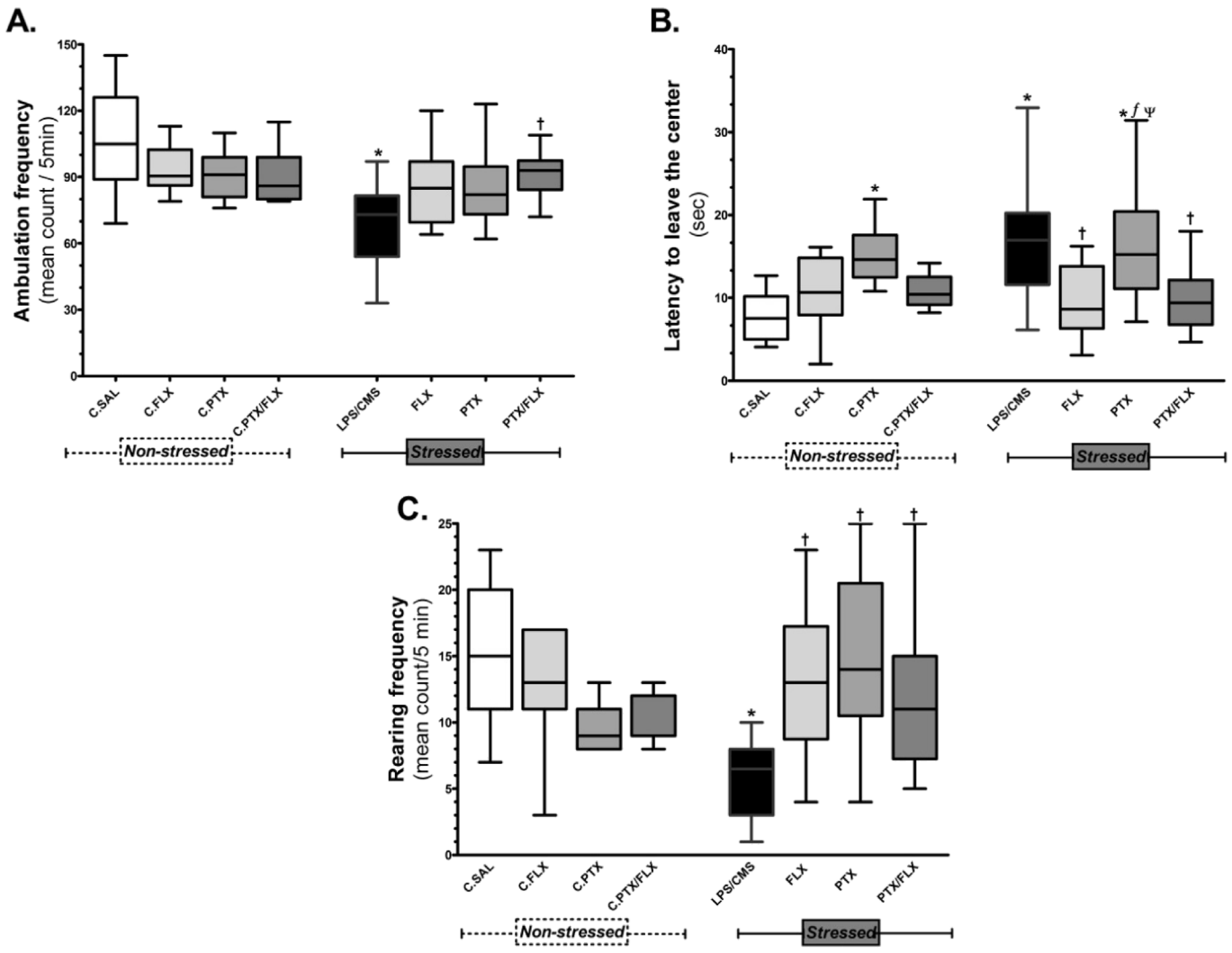

Fig. 9. Effects of FLX and PTX treatment either alone or in combination on the behavioral changes in open field test.
Box-Whisker graph illustrating changes in the OFT in *rats exposed to different stressful protocols;* **(A) Total ambulation**; **(B) Latency to leave the center zone**; **(C) Rearing**. Data are presented as median/interquartile range. C.SAL (n = 11), C.FLX (n = 9), C.PTX (n = 11), C.PTX/FLX (n = 11), LPS/CMS (n = 18), LPS/SAL-FLX (n = 18), LPS/SAL-PTX (n = 17), LPS/SAL-PTX/FLX (n = 16). For comparisons among groups Kruskal-Wallis Test followed by post hoc "Dunn's Multiple Comparisons Test" was utilized. $^{*}p < 0.05$ significant in comparison to C.SAL, $^{\dagger}p < 0.05$ significant in comparison to the LPS/CMS, $^{f}p < 0.05$ in comparison to LPS/CMS-FLX, < SUP > Ψ < /SUP > $p < 0.05$ in comparison to LPS/CMS-PTX/FLX.**Non-stressed:** Control groups not subjected to stress; **Stressed:** Challenged with the combined LPS/CMS model; **C.SAL:** Control saline; **FLX:** Fluoxetine (10 mg/kg i.p.); **PTX:** Pentoxiphylline (100 mg/kg i.p.); **LPS:** Lipopolysaccharides (50 μg/kg i.p., every other day, a total of six doses); **CMS:** Chronic mild stress (4 weeks).

mitochondrial biogenesis may maintain homeostasis via supporting metabolic functions and cell viability [82]. Among the variety of signaling pathways, PGC1-α, has been identified as a crucial coordinator of mitochondrial biogenesis in response to stressful stimuli [8,83]. Downstream of PGC-1α, the nuclear transcription factor NRF-1 [16,83] which up-regulates the mitochondrial transcription factor TFAM that is essential for the initiation of mt-DNA replication [83]. Indeed, in the present study, (LPS/CMS) showed a significant decrease in the expression of the PGC1-α, NRF1, TFAM as well as the mt-DNA copy number; reflecting a deficiency in the mitochondrial biogenesis machinery. These novel findings in an animal model of depression are in harmony with recent reports that observed the association of altered mt-DNA content with disturbed mitochondrial functions in depressed patients [84–87]. In this vein of special relevance, Kim et al. associated decreased mt-DNA content with depression in old women [86]. Such findings propose that mt-DNA content may be a useful marker of mitochondrial dysfunction and the defective repair mechanisms (particularly mitochondrial biogenesis) in stress-induced depressive disorder.

Interestingly, the attenuation of the TLR4/NFκB signaling via FLX, PTX and PTX/FLX prevented the LPS/CMS-induced downregulation of PGC-1α and its consequent mitochondrial biogenesis machinery. This came in agreement with earlier studies reporting the association of TLR4/NFκB, activation and the repression of genes encoding PGC-1α [88] and the enhancement of mitochondrial dysfunction [89].

An intricate inter-relationship exists between the PGC-1α mediated transcriptional control of mitochondrial biogenesis and crucial metabolic signaling pathways [8,83]. In fact, cellular energy deficit manifested by an increase in the AMP/ATP ratio induce PGC-1α phosphorylation via the metabolic sensor AMPK [90]. An additional metabolic marker assuring the energy deficit state in the stressed rats was AEC. Notably, AEC ratio represents the amount of the metabolically available energy which is stored in the TAN pool [42]. Accordingly, AEC value provides a quantitative assessment of the cellular energy status. In conditions of homeostasis, AEC is strictly controlled with values ranging from 0.5 to 0.9 indicative of healthy cells. Values of 0.55–0.75 indicate the negative effect of a stress factor inducing the consumption of energy for defense mechanisms, whereas values below 0.5 accompany cell death [43]. Consequently, it is expected that in presence of

any metabolic stress and higher energy requirement, that cells will react with a depletion of ATP and a simultaneous increase in the AMP levels and a significant decrease of AEC [44]. Noteworthy, in the current investigation, LPS/CMS stressed hippocampal tissue showed a decline in the energy status, manifested as a decrease in AEC (0.56) paralleled with an increase in AMP/ATP ratio and p-AMPK, indicating high metabolic stress (Table 5**).**

Inconsistently, in the present study the LPS/CMS-induced increase in the AMP/ATP ratio and p-AMPK **(**Table 5**)** were corroborated with a paradoxical decline in PGC1-α, NRF1, TFAM and mt-DNA content (Fig. 5a**)**. A plausible explanation for this paradoxic finding may be attributed to the notion that p-AMPK may exhibit a bidirectional response via either favoring mitophagy (the destruction of defective mitochondria) or mitochondrial biogenesis. This may be attributed to the fact that AMPK serve as a link between PGC-1α regulated mitochondrial biogenesis and the target of rapamycin complex 1 (TORC1) [91–94]. Accordingly, it may be assumed that AMPK is a double edged metabolic sensor; where it could enhance the synthesis of new mitochondria through its activation of PGC-1α and at the same time promote the clearance of defective mitochondria while suppressing cell growth. In a further support for the probable link between highly elevated p-AMPK and mitochondrial loss and the consequent induction of depressive [95], reported that sustained AMPK activation might be a mechanism by which chronic CORT treatment causes depressive-like behavior in male mice. These findings fall in line with the chronic elevation of serum CORT (Table 6**)** observed in the LPS/CMS group. Furthermore, our findings are in line with Schilling et al. [88], who reported that LPS-induced stimulation of the TLR4/NFκB was associated with an elevation of p-AMPK and a down regulation of PGC1-α, arguing that AMPK is not upstream of the metabolic regulation manifested by PGC1-α.

In a previous study we reported that CMS was associated with hippocampal apoptosis and impaired energy metabolism [11] manifested by AEC below 0.55 that was successfully enhanced upon paroxetine treatment. Indeed, in the present study, rats treated with FLX, PTX as well as their combination showed a decline in the p-AMPK level that was accompanied by a further improvement in the cellular energy status as manifested via the increase AEC and the decrease in AMP/ATP ratio as well as was an increase in the expression of PGC1-α, NRF-1, TFAM and mt-DNA. Thus, down-regulation of the p-AMPK may have a neuroprotective role (Table 6**)**. Notably, Venna et al. reported that down-regulation of p-AMPK contributed to the neuroprotective effects of ischemic preconditioning, an effect that was obliterated in AMPK knockout mice [96].

Apart from the stress-induced quantitative deficiency of the mitochondrial content, another structural mitochondrial imperfection was also observed in this study. Electron microscopy examination showed mitochondrial membrane structural changes as well as distorted reminiscent cristae in electron micrographs **(**Figs. 3b **and** 5b**).** This finding is consistent with that from a previous reported by Gong et al. associating mitochondrial dysfunction and ultra-structural damage in the hippocampus of rats exposed to CMS [97]. Accordingly, the aforementioned findings extend our previous observations that chronic stress induced depressive behavior was associated with apoptosis and deranged energy metabolism [11], to further include altered transcriptional, structural, and functional mitochondrial activity as other members in the scenario of the stress-induced problematic mitochondria.

It's relevant to note that the enhanced antidepressant behavioral effects observed by the combined treatment (PTX/FLX) may be attributed to the interactions among monoamines, mitochondrial functions and inflammation; as previously suggested by Gardner and Boles [9]. A finding that could lend further credence to what was reported in our lab, regarding the efficacy of adding PTX to the SSRI “escitalopram” *(vide supra)*. The observed augmentation in the enhancement of the markers of mitochondrial biogenesis as well as the improvement of the hippocampal energy status offered by adding PTX to FLX treatment in the presented study, would highly implicate such a combination in the treatment of MDD patients.

5. Conclusion

Taken all together, we can presume that mitochondrial abnormalities may be a contingent factor in stress-induced depression and altered cerebral energy metabolism. These observations may nominate the mitochondrial targeted pathway as a promising gateway therapy for providing neuroprotection. Indeed, in our study we proposed that the combined stress model LPS/CMS prompted an initial cross talk between the activated TLR4-dependnt NFκB and the consequent suppression of the PGC1-α induced regulation of mitochondrial biogenesis and energy metabolism. FLX and PTX treatment reversed the TLR4-induced energy metabolic reprogramming via enhancement of the PGC1-α/NRF1/TFAM signaling independent on the metabolic energy sensor p-AMPk.

Declaration of competing interest

The authors declare that there are no conflicts of interest.

References

[1] R. Dantzer, J.C. O'Connor, G.G. Freund, R.W. Johnson, K.W. Kelley, From inflammation to sickness and depression: when the immune system subjugates the brain, Nat. Rev. Neurosci. 9 (1) (2008) 46–56.
[2] M.-C. Audet, R.J. McQuaid, Z. Merali, H. Anisman, Cytokine variations and mood disorders: influence of social stressors and social support, Front. Neurosci. 8 (2014) 416.
[3] B. Garcia-Bueno, J.R. Caso, J.C. Leza, Stress as a neuroinflammatory condition in brain: damaging and protective mechanisms, Neurosci. Biobehav. Rev. 32 (6) (2008) 1136–1151.
[4] J. Liu, F. Buisman-Pijlman, M.R. Hutchinson, Toll-like receptor 4: innate immune regulator of neuroimmune and neuroendocrine interactions in stress and major depressive disorder, Front. Neurosci. 8 (2014) 309.
[5] M. Maes, R. Yirmyia, J. Noraberg, S. Brene, J. Hibbeln, G. Perini, M. Kubera, P. Bob, B. Lerer, M. Maj, The inflammatory & neurodegenerative (I&ND) hypothesis of depression: leads for future research and new drug developments in depression, Metab. Brain Dis. 24 (1) (2009) 27–53.
[6] C.L. Raison, L. Capuron, A.H. Miller, Cytokines sing the blues: inflammation and the pathogenesis of depression, Trends Immunol. 27 (1) (2006) 24–31.
[7] L. Capuron, A.H. Miller, Immune system to brain signaling: neuropsychopharmacological implications, Pharmacol. Ther. 130 (2) (2011) 226–238.
[8] A.D. Cherry, C.A. Piantadosi, Regulation of mitochondrial biogenesis and its intersection with inflammatory responses, Antioxidants Redox Signal. 22 (12) (2015) 965–976.
[9] A. Gardner, R.G. Boles, Beyond the serotonin hypothesis: mitochondria, inflammation and neurodegeneration in major depression and affective spectrum disorders, Prog. Neuro-Psychopharmacol. Biol. Psychiatry 35 (3) (2011) 730–743.
[10] S. Aboul-Fotouh, Chronic treatment with coenzyme Q10 reverses restraint stress-induced anhedonia and enhances brain mitochondrial respiratory chain and creatine kinase activities in rats, Behav. Pharmacol. 24 (7) (2013) 552–560.
[11] L.H. Khedr, N.N. Nassar, E.S. El-Denshary, A.M. Abdel-Tawab, Paroxetine ameliorates changes in hippocampal energy metabolism in chronic mild stress-exposed rats, Neuropsychiatric Dis. Treat. 11 (2015) 2887–2901.
[12] J.L. Madrigal, R. Olivenza, M.A. Moro, I. Lizasoain, P. Lorenzo, J. Rodrigo, J.C. Leza, Glutathione depletion, lipid peroxidation and mitochondrial dysfunction are induced by chronic stress in rat brain, Neuropsychopharmacology : Off. Publ. Am. Coll. Neuropsychopharmacol. 24 (4) (2001) 420–429.
[13] G.T. Rezin, M.R. Cardoso, C.L. Goncalves, G. Scaini, D.B. Fraga, R.E. Riegel, C.M. Comim, J. Quevedo, E.L. Streck, Inhibition of mitochondrial respiratory chain in brain of rats subjected to an experimental model of depression, Neurochem. Int. 53 (6–8) (2008) 395–400.
[14] B. Tagliari, C.G. Noschang, A.G. Ferreira, O.A. Ferrari, L.R. Feksa, C.M. Wannmacher, C. Dalmaz, A.T. Wyse, Chronic variable stress impairs energy metabolism in prefrontal cortex and hippocampus of rats: prevention by chronic antioxidant treatment, Metab. Brain Dis. 25 (2) (2010) 169–176.
[15] R. Anne Stetler, R.K. Leak, Y. Gao, J. Chen, The dynamics of the mitochondrial organelle as a potential therapeutic target, J. Cereb. Blood Flow Metab. 33 (1) (2013) 22–32.
[16] I. Manoli, S. Alesci, M.R. Blackman, Y.A. Su, O.M. Rennert, G.P. Chrousos, Mitochondria as key components of the stress response, Trends Endocrinol. Metab.: TEM (Trends Endocrinol. Metab.) 18 (5) (2007) 190–198.
[17] R.A. Stetler, R.K. Leak, W. Yin, L. Zhang, S. Wang, Y. Gao, J. Chen, Mitochondrial biogenesis contributes to ischemic neuroprotection afforded by LPS pre-conditioning, J. Neurochem. 123 (Suppl 2) (2012) 125–137.
[18] T. Wenz, Regulation of mitochondrial biogenesis and PGC-1Î ± under cellular stress, Mitochondrion (0) (2013).
[19] M. Maes, M. Kubera, J.C. Leunis, M. Berk, Increased IgA and IgM responses against

gut commensals in chronic depression: further evidence for increased bacterial translocation or leaky gut, J. Affect. Disord. 141 (1) (2012) 55–62.
[20] I. Garate, B. Garcia-Bueno, J.L. Madrigal, L. Bravo, E. Berrocoso, J.R. Caso, J.A. Mico, J.C. Leza, Origin and consequences of brain Toll-like receptor 4 pathway stimulation in an experimental model of depression, J. Neuroinflammation 8 (2011) 151.
[21] J.C. O'Connor, C. Andre, Y. Wang, M.A. Lawson, S.S. Szegedi, J. Lestage, N. Castanon, K.W. Kelley, R. Dantzer, Interferon-gamma and tumor necrosis factor-alpha mediate the upregulation of indoleamine 2,3-dioxygenase and the induction of depressive-like behavior in mice in response to bacillus Calmette-Guerin, J. Neurosci. : Off. J. Soc. Neurosci. 29 (13) (2009) 4200–4209.
[22] J.C. O'Connor, M.A. Lawson, C. Andre, M. Moreau, J. Lestage, N. Castanon, K.W. Kelley, R. Dantzer, Lipopolysaccharide-induced depressive-like behavior is mediated by indoleamine 2,3-dioxygenase activation in mice, Mol. Psychiatry 14 (5) (2009) 511–522.
[23] R. De, La Garza Ii, Endotoxin- or pro-inflammatory cytokine-induced sickness behavior as an animal model of depression: focus on anhedonia, Neurosci. Biobehav. Rev. 29 (4â€“5) (2005) 761–770.
[24] F. Frenois, M. Moreau, J. O'Connor, M. Lawson, C. Micon, J. Lestage, K.W. Kelley, R. Dantzer, N. Castanon, Lipopolysaccharide induces delayed FosB/DeltaFosB immunostaining within the mouse extended amygdala, hippocampus and hypothalamus, that parallel the expression of depressive-like behavior, Psychoneuroendocrinol 32 (2007) 516–531.
[25] A.S. Elgarf, S. Aboul-Fotouh, H.A. Abd-Alkhalek, M. El Tabbal, A.N. Hassan, S.K. Kassim, G.A. Hammouda, K.A. Farrag, A.M. Abdel-tawab, Lipopolysaccharide repeated challenge followed by chronic mild stress protocol introduces a combined model of depression in rats: reversibility by imipramine and pentoxifylline, Pharmacol. Biochem. Behav. 126 (2014) 152–162.
[26] Y. Ohgi, T. Futamura, T. Kikuchi, K. Hashimoto, Effects of antidepressants on alternations in serum cytokines and depressive-like behavior in mice after lipopolysaccharide administration, Pharmacol. Biochem. Behav. 103 (4) (2013) 853–859.
[27] C. Roumestan, A. Michel, F. Bichon, K. Portet, M. Detoc, C. Henriquet, D. Jaffuel, M. Mathieu, Anti-inflammatory properties of desipramine and fluoxetine, Respir. Res. 8 (2007) 35.
[28] R. Yirmiya, Y. Pollak, O. Barak, R. Avitsur, H. Ovadia, M. Bette, E. Weihe, J. Weidenfeld, Effects of antidepressant drugs on the behavioral and physiological responses to lipopolysaccharide (LPS) in rodents, Neuropsychopharmacology : Off. Publ. Am. Coll. Neuropsychopharmacol. 24 (5) (2001) 531–544.
[29] B. Leonard, M. Maes, Mechanistic explanations how cell-mediated immune activation, inflammation and oxidative and nitrosative stress pathways and their sequels and concomitants play a role in the pathophysiology of unipolar depression, Neurosci. Biobehav. Rev. 36 (2) (2012) 764–785.
[30] S. Keri, C. Szabo, O. Kelemen, Expression of Toll-Like Receptors in peripheral blood mononuclear cells and response to cognitive-behavioral therapy in major depressive disorder, Brain Behav. Immun. 40 (2014) 235–243.
[31] M.-K. Wu, T.-L. Huang, K.-W. Huang, Y.-L. Huang, Y.-Y. Hung, Association between toll-like receptor 4 expression and symptoms of major depressive disorder, Neuropsychiatric Dis. Treat. 11 (2015) 1853–1857.
[32] S. Biesmans, J.A. Bouwknecht, L. Ver Donck, X. Langlois, P.D. Acton, P. De Haes, N. Davoodi, T.F. Meert, N. Hellings, R. Nuydens, Peripheral administration of tumor necrosis factor-alpha induces neuroinflammation and sickness but not depressive-like behavior in mice, BioMed Res. Int. 2015 (2015) 716920.
[33] C.A. Browne, F.E. O'Brien, T.J. Connor, T.G. Dinan, J.F. Cryan, Differential lipopolysaccharide-induced immune alterations in the hippocampus of two mouse strains: effects of stress, Neuroscience 225 (2012) 237–248.
[34] S.T. Anderson, S. Commins, P. Moynagh, A.N. Coogan, Chronic fluoxetine treatment attenuates post-septic affective changes in the mouse, Behav. Brain Res. 297 (2016) 112–115.
[35] I.S. Oliveira-Junior, W.R. Oliveira, S.S. Cavassani, M.K. Brunialti, R. Salomao, Effects of pentoxifylline on inflammation and lung dysfunction in ventilated septic animals, J. Trauma 68 (4) (2010) 822–826.
[36] B.M. Mohamed, S. Aboul-Fotouh, E.A. Ibrahim, H. Shehata, A.A. Mansour, N.A. Yassin, W. El-Eraky, A.M. Abdel-Tawab, Effects of pentoxifylline, 7-nitroindazole, and imipramine on tumor necrosis factor-alpha and indoleamine 2,3-dioxygenase enzyme activity in the hippocampus and frontal cortex of chronic mild-stress-exposed rats, Neuropsychiatric Dis. Treat. 9 (2013) 697–708.
[37] ILAR (Institute of Laboratory Animal Resources), Guide for the Care and Use of Laboratory Animals. NIH Publication No. 85-23 (Revised 1996), National Academy Press, Washington, D.C, 1996.
[38] A.J. Grippo, T.G. Beltz, R.M. Weiss, A.K. Johnson, The effects of chronic fluoxetine treatment on chronic mild stress-induced cardiovascular changes and anhedonia, Biol. Psychiatry 59 (4) (2006) 309–316.
[39] A. Colson, B. Willems, J.P. Thissen, Inhibition of TNF-alpha production by pentoxifylline does not prevent endotoxin-induced decrease in serum IGF-I, J. Endocrinol. 178 (1) (2003) 101–109.
[40] F.F. Tukov, J.P. Luyendyk, P.E. Ganey, R.A. Roth, The role of tumor necrosis factor alpha in lipopolysaccharide/ranitidine-induced inflammatory liver injury, Toxicol. Sci. : Off. J. Soc. Toxicol. 100 (1) (2007) 267–280.
[41] R.C. Gupta, W.D. Dettbarn, Prevention of kainic acid seizures-induced changes in levels of nitric oxide and high-energy phosphates by 7-nitroindazole in rat brain regions, Brain Res. 981 (1–2) (2003) 184–192.
[42] I. Baranowska-Bosiacka, I. Gutowska, C. Marchetti, M. Rutkowska, M. Marchlewicz, A. Kolasa, A. Prokopowicz, I. Wiernicki, K. Piotrowska, M. Baskiewicz, K. Safranow, B. Wiszniewska, D. Chlubek, Altered energy status of primary cerebellar granule neuronal cultures from rats exposed to lead in the pre- and neonatal period, Toxicology 280 (1–2) (2011) 24–32.
[43] Z. Din, J. Brooks, Use of adenylate energy charge as a physiological indicator in toxicity experiments, Bull. Environ. Contam. Toxicol. 36 (1) (1986) 1–8.
[44] D.E. Atkinson, The energy charge of the adenylate pool as a regulatory parameter. Interaction with feedback modifiers, Biochemistry 7 (11) (1968) 4030–4034.
[45] C. Canto, J. Auwerx, PGC-1alpha, SIRT1 and AMPK, an energy sensing network that controls energy expenditure, Curr. Opin. Lipidol. 20 (2) (2009) 98–105.
[46] P. Willner, Chronic mild stress (CMS) revisited: consistency and behavioural-neurobiological concordance in the effects of CMS, Neuropsychobiology 52 (2) (2005) 90–110.
[47] S. Chiba, T. Numakawa, M. Ninomiya, M.C. Richards, C. Wakabayashi, H. Kunugi, Chronic restraint stress causes anxiety- and depression-like behaviors, downregulates glucocorticoid receptor expression, and attenuates glutamate release induced by brain-derived neurotrophic factor in the prefrontal cortex, Prog. Neuro-Psychopharmacol. Biol. Psychiatry 39 (1) (2012) 112–119.
[48] S. Bekris, K. Antoniou, S. Daskas, Z. Papadopoulou-Daifoti, Behavioural and neurochemical effects induced by chronic mild stress applied to two different rat strains, Behav. Brain Res. 161 (1) (2005) 45–59.
[49] R.D. Porsolt, M. Le Pichon, M. Jalfre, Depression: a new animal model sensitive to antidepressant treatments, Nature 266 (5604) (1977) 730–732.
[50] V. Castagne, P. Moser, S. Roux, R.D. Porsolt, Rodent models of depression: forced swim and tail suspension behavioral despair tests in rats and mice, Curr. Protoc. Neurosci. Chapter 8 (2011) Unit 8 10A..
[51] K. Nosek, K. Dennis, B.M. Andrus, N. Ahmadiyeh, A.E. Baum, L.C. Solberg Woods, E.E. Redei, Context and strain-dependent behavioral response to stress, Behav. Brain Funct. : BBF 4 (2008) 23.
[52] G. Paxinos, C. Watson, The Rat Brain in Stereotaxic Coordinates, sixth ed., Elsevier, 2007.
[53] A. Arjona, D.K. Sarkar, Circadian oscillations of clock genes, cytolytic factors, and cytokines in rat NK cells, J. Immunol. 174 (12) (2005) 7618–7624.
[54] J.M. Duhart, M.J. Leone, N. Paladino, J.A. Evans, O. Castanon-Cervantes, A.J. Davidson, D.A. Golombek, Suprachiasmatic astrocytes modulate the circadian clock in response to TNF-alpha, J. Immunol. 191 (9) (2013) 4656–4664.
[55] Z. Guan, A.N. Vgontzas, T. Omori, X. Peng, E.O. Bixler, J. Fang, Interleukin-6 levels fluctuate with the light-dark cycle in the brain and peripheral tissues in rats, Brain Behav. Immun. 19 (6) (2005) 526–529.
[56] I. Kolbe, R. Dumbell, H. Oster, Circadian clocks and the interaction between stress Axis and adipose function, Int. J. Endocrinol. 2015 (2015) 693204.
[57] L. Marpegan, T.A. Bekinschtein, M.A. Costas, D.A. Golombek, Circadian responses to endotoxin treatment in mice, J. Neuroimmunol. 160 (1–2) (2005) 102–109.
[58] A.E. Franklin, C.G. Engeland, M. Kavaliers, K.P. Ossenkopp, Lipopolysaccharide-induced hypoactivity and behavioral tolerance development are modulated by the light-dark cycle in male and female rats, Psychopharmacology 170 (4) (2003) 399–408.
[59] J.D. Morrow, M.R. Opp, Diurnal variation of lipopolysaccharide-induced alterations in sleep and body temperature of interleukin-6-deficient mice, Brain Behav. Immun. 19 (1) (2005) 40–51.
[60] C. Bielajew, A.T. Konkle, Z. Merali, The effects of chronic mild stress on male Sprague-Dawley and Long Evans rats: I. Biochemical and physiological analyses, Behav. Brain Res. 136 (2) (2002) 583–592.
[61] P.S. D'Aquila, A.T. Peana, V. Carboni, G. Serra, Exploratory behaviour and grooming after repeated restraint and chronic mild stress: effect of desipramine, Eur. J. Pharmacol. 399 (1) (2000) 43–47.
[62] G. Lucca, C.M. Comim, S.S. Valvassori, G.Z. Reus, F. Vuolo, F. Petronilho, E.C. Gavioli, F. Dal-Pizzol, J. Quevedo, Increased oxidative stress in submitochondrial particles into the brain of rats submitted to the chronic mild stress paradigm, J. Psychiatr. Res. 43 (9) (2009) 864–869.
[63] R. Muscat, P. Willner, Suppression of sucrose drinking by chronic mild unpredictable stress: a methodological analysis, Neurosci. Biobehav. Rev. 16 (4) (1992) 507–517.
[64] R.J. Katz, K.A. Roth, B.J. Carroll, Acute and chronic stress effects on open field activity in the rat: implications for a model of depression, Neurosci. Biobehav. Rev. 5 (2) (1981) 247–251.
[65] M. Tonissaar, T. Mallo, M. Eller, R. Haidkind, K. Koiv, J. Harro, Rat behavior after chronic variable stress and partial lesioning of 5-HT-ergic neurotransmission: effects of citalopram, Prog. Neuro-Psychopharmacol. Biol. Psychiatry 32 (1) (2008) 164–177.
[66] G. Ping, W. Qian, G. Song, S. Zhaochun, Valsartan reverses depressive/anxiety-like behavior and induces hippocampal neurogenesis and expression of BDNF protein in unpredictable chronic mild stress mice, Pharmacol. Biochem. Behav. 124 (2014) 5–12.
[67] S. Akira, S. Uematsu, O. Takeuchi, Pathogen recognition and innate immunity, Cell 124 (2006) 783–801.
[68] J. Caso, J. Pradillo, O. Hurtado, P. Lorenzo, M. Moro, I. Lizasoain, Toll-like receptor 4 is involved in brain damage and inflammation after experimental stroke, Circulation 115 (2007) 1599–1608.
[69] M. Maes, M. Kubera, J.C. Leunis, The gut-brain barrier in major depression: intestinal mucosal dysfunction with an increased translocation of LPS from gram negative enterobacteria (leaky gut) plays a role in the inflammatory pathophysiology of depression, Neuroendocrinol. Lett. 29 (1) (2008) 117–124.
[70] J.R. Caso, J.M. Pradillo, O. Hurtado, J.C. Leza, M.A. Moro, I. Lizasoain, Toll-like receptor 4 is involved in subacute stress-induced neuroinflammation and in the worsening of experimental stroke, Stroke, J. Cereb. Circ. 39 (4) (2008) 1314–1320.
[71] S. Akira, K. Takeda, Toll-like receptor signaling, Nat. Rev. Immunol. 4 (2004) 499–511.
[72] G. Gong, S. Bai, W. Wu, L. Hu, Y. Liu, J. Niu, X. Dai, L. Yin, X. Wang, Lrg participates in lipopolysaccharide preconditioning-induced brain ischemia injury via TLR4

signaling pathway, J. Mol. Neurosci. : MN 54 (1) (2014) 20–26.
[73] M.P. Kaster, V.M. Gadotti, J.B. Calixto, A.R. Santos, A.L. Rodrigues, Depressive-like behavior induced by tumor necrosis factor-alpha in mice, Neuropharmacology 62 (1) (2012) 419–426.
[74] J.W. Koo, S.J. Russo, D. Ferguson, E.J. Nestler, R.S. Duman, Nuclear factor-kappaB is a critical mediator of stress-impaired neurogenesis and depressive behavior, Proc. Natl. Acad. Sci. U. S. A 107 (6) (2010) 2669–2674.
[75] I. Gárate, B. García-Bueno, J.L.M. Madrigal, J.R. Caso, L. Alou, M.L. Gómez-Lus, J.C. Leza, Toll-like 4 receptor inhibitor TAK-242 decreases neuroinflammation in rat brain frontal cortex after stress, J. Neuroinflammation 11 (2014) 8-8..
[76] C.-M. Lim, S.-W. Kim, J.-Y. Park, C. Kim, S.H. Yoon, J.-K. Lee, Fluoxetine affords robust neuroprotection in the postischemic brain via its anti-inflammatory effect, J. Neurosci. Res. 87 (4) (2009) 1037–1045.
[77] C.C. Barton, E.X. Barton, P.E. Ganey, S.L. Kunkel, R.A. Roth, Bacterial lipopolysaccharide enhances aflatoxin B1 hepatotoxicity in rats by a mechanism that depends on tumor necrosis factor alpha, Hepatology (Baltimore, Md 33 (1) (2001) 66–73.
[78] B.J. Dezube, M.L. Sherman, J.L. Fridovich-Keil, J. Allen-Ryan, A.B. Pardee, Down-regulation of tumor necrosis factor expression by pentoxifylline in cancer patients: a pilot study, Cancer immunology, immunotherapy, CII 36 (1) (1993) 57–60.
[79] S.C. Correia, C. Carvalho, S. Cardoso, R.X. Santos, M.S. Santos, C. Oliveira, G. Perry, X. Zhu, M.A. Smith, P.I. Moreira, Mitochondrial preconditioning: a potential neuroprotective strategy, Front. Aging Neurosci. 2 (2010).
[80] D.R. Gutsaeva, M.S. Carraway, H.B. Suliman, I.T. Demchenko, H. Shitara, H. Yonekawa, C.A. Piantadosi, Transient hypoxia stimulates mitochondrial biogenesis in brain subcortex by a neuronal nitric oxide synthase-dependent mechanism, J. Neurosci. : Off. J. Soc. Neurosci. 28 (9) (2008) 2015–2024.
[81] B. Marsh, S.L. Stevens, A.E. Packard, B. Gopalan, B. Hunter, P.Y. Leung, C.A. Harrington, M.P. Stenzel-Poore, Systemic lipopolysaccharide protects the brain from ischemic injury by reprogramming the response of the brain to stroke: a critical role for IRF3, J. Neurosci. : Off. J. Soc. Neurosci. 29 (31) (2009) 9839–9849.
[82] C.A. Piantadosi, H.B. Suliman, Transcriptional control of mitochondrial biogenesis and its interface with inflammatory processes, Biochim. Biophys. Acta 1820 (4) (2012) 532–541.
[83] R.C. Scarpulla, R.B. Vega, D.P. Kelly, Transcriptional integration of mitochondrial biogenesis, Trends Endocrinol. Metab.: TEM (Trends Endocrinol. Metab.) 23 (9) (2012) 459–466.
[84] C.C. Chang, S.H. Jou, T.T. Lin, T.J. Lai, C.S. Liu, Mitochondria DNA change and oxidative damage in clinically stable patients with major depressive disorder, PLoS One 10 (5) (2015) e0125855.
[85] A. Gardner, A. Johansson, R. Wibom, I. Nennesmo, U. von Dobeln, L. Hagenfeldt, T. Hallstrom, Alterations of mitochondrial function and correlations with personality traits in selected major depressive disorder patients, J. Affect. Disord. 76 (1–3) (2003) 55–68.
[86] M.Y. Kim, J.W. Lee, H.C. Kang, E. Kim, D.C. Lee, Leukocyte mitochondrial DNA (mtDNA) content is associated with depression in old women, Arch. Gerontol. Geriatr. 53 (2) (2011) e218–e221.
[87] A.N. Malik, A. Czajka, Is mitochondrial DNA content a potential biomarker of mitochondrial dysfunction? Mitochondrion 13 (5) (2013) 481–492.
[88] J. Schilling, L. Lai, N. Sambandam, C.E. Dey, T.C. Leone, D.P. Kelly, Toll-like receptor-mediated inflammatory signaling reprograms cardiac energy metabolism by repressing peroxisome proliferator-activated receptor gamma coactivator-1 signaling, Circulation, Heart Fail. 4 (4) (2011) 474–482.
[89] S. Yuan, X. Liu, X. Zhu, Z. Qu, Z. Gong, J. Li, L. Xiao, Y. Yang, H. Liu, L. Sun, F. Liu, The role of TLR4 on PGC-1alpha-mediated oxidative stress in tubular cell in diabetic kidney disease, oxidative medicine and cellular longevity 2018, (2018), p. 6296802.
[90] S. Jager, C. Handschin, J. St-Pierre, B.M. Spiegelman, AMP-activated protein kinase (AMPK) action in skeletal muscle via direct phosphorylation of PGC-1alpha, Proc. Natl. Acad. Sci. U. S. A 104 (29) (2007) 12017–12022.
[91] D.M. Gwinn, D.B. Shackelford, D.F. Egan, M.M. Mihaylova, A. Mery, D.S. Vasquez, B.E. Turk, R.J. Shaw, AMPK phosphorylation of raptor mediates a metabolic checkpoint, Mol. Cell 30 (2) (2008) 214–226.
[92] K. Inoki, T. Zhu, K.L. Guan, TSC2 mediates cellular energy response to control cell growth and survival, Cell 115 (5) (2003) 577–590.
[93] D.F. Egan, D.B. Shackelford, M.M. Mihaylova, S. Gelino, R.A. Kohnz, W. Mair, D.S. Vasquez, A. Joshi, D.M. Gwinn, R. Taylor, J.M. Asara, J. Fitzpatrick, A. Dillin, B. Viollet, M. Kundu, M. Hansen, R.J. Shaw, Phosphorylation of ULK1 (hATG1) by AMP-activated protein kinase connects energy sensing to mitophagy, Science 331 (6016) (2011) 456–461.
[94] J. Kim, M. Kundu, B. Viollet, K.L. Guan, AMPK and mTOR regulate autophagy through direct phosphorylation of Ulk1, Nat. Cell Biol. 13 (2) (2011) 132–141.
[95] Y. Zhao, J. Shen, H. Su, B. Li, D. Xing, L. Du, Chronic corticosterone injections induce a decrease of ATP levels and sustained activation of AMP-activated protein kinase in hippocampal tissues of male mice, Brain Res. 1191 (2008) 148–156.
[96] V.R. Venna, J. Li, S.E. Benashski, S. Tarabishy, L.D. McCullough, Preconditioning induces sustained neuroprotection by down regulation of AMPK, Neuroscience 201 (2012) 280–287.
[97] Y. Gong, Y. Chai, J.H. Ding, X.L. Sun, G. Hu, Chronic mild stress damages mitochondrial ultrastructure and function in mouse brain, Neurosci. Lett. 488 (1) (2011) 76–80.